Modular Space Vehicle Architecture for Human Exploration of Mars Using Artificial Gravity and Mini-Magnetosphere Crew...

Article *in* AIAA Journal · January 2012

DOI: 10.2514/6.2012-633

6 authors, including:

Ruth A. Bamford
Science and Technology Facilities Council
61 PUBLICATIONS **218** CITATIONS
SEE PROFILE

Robin Stafford-Allen
Culham Centre for Fusion Energy
13 PUBLICATIONS **31** CITATIONS
SEE PROFILE

50th AIAA Aerospace Sciences Meeting including the New Horizons Forum and Aerospace Exposition
09 - 12 January 2012, Nashville, Tennessee

AIAA 2012-0633

Modular Space Vehicle Architecture for Human Exploration of Mars using Artificial Gravity and Mini-Magnetosphere Crew Radiation Shield

Mark G. Benton, Sr.[*]
The Boeing Company, El Segundo, CA 90009-2919, USA

Bernard Kutter[†]
United Launch Alliance, Denver CO, USA

Dr. Ruth A. Bamford[‡] and Prof. Bob Bingham[§]
RAL Space, Rutherford Appleton Laboratory, Chilton, Didcot, OX13 6BL, U.K

and

Tom Todd[**] and Robin Stafford-Allen[††]
Culham Centre for Fusion Energy, Culham Science Centre, Abingdon, OX14 3DB, U.K.

This paper presents a conceptual Mars Exploration Vehicle (MEV) architecture, which includes two unmanned Mars Lander Transfer Vehicles (MLTVs) and a Mars Crew Transfer Vehicle (MCTV) with a crew of four. The MLTVs and MCTV are assembled in low Earth orbit (LEO) from modules launched by four Space Launch System (SLS) and five Delta IV Heavy rockets. The MLTVs and MCTV individually escape from LEO, transit to Mars, brake into Mars orbit using propulsion and aerobraking, and rendezvous and dock in low Mars orbit (LMO). Each MLTV includes an Earth Departure stage (EDS), Mars Transfer Stage (MTS), Lander Service Module (LSM), and two landers: A Mars Personnel Lander (MPL) provides two-way crew transportation between LMO and the surface. Three unmanned Mars Cargo Landers (MCLs) provide one-way cargo transportation and the functionalities of habitats (MCL-H) (2) and rover (MCL-R). The landers rendezvous and assemble on the surface to form a base. The MCTV includes two EDS, two MTS, and the following: (1) The Multi-Purpose Crew Vehicle (MPCV) transports the crew from Earth to LEO, provides propulsion, and returns the crew to Earth after nominal mission completion or in aborts. (2) Three Deep Space Vehicles (DSVs) provide life support consumables, passive biological radiation shielding, crew habitation space, and propulsion. The DSV design was derived from the MCL-H. (3) An Artificial Gravity Module (AGM) allows the MCTV to rotate and generate artificial gravity for the crew and provides photo-voltaic power generation and deep space communications. A miniature magnetosphere (Mini-Mag), a potential key enabler for human interplanetary exploration, is electromagnetically generated on the AGM and provides active crew biological radiation shielding. The MEV architecture is based on many existing or near-term technologies. It incorporates significant modularity and could provide an economical approach to achieve progressively more ambitious stepping stone missions along a flexible path for human solar system exploration: starting with test flights in Earth and lunar orbit and progressing through missions to near-Earth asteroids and the moons of Mars, and culminating in the Mars landing mission.

[*] Boeing Company, Mail Code W-S50-X403, POB 92919, Los Angeles, CA 90009-2919. Senior Member of AIAA.
[†] Manager, Advanced Programs, United Launch Alliance
[‡] Also at: Department of Physics, University of York, Heslington, York, YO10 5DD, UK.
[§] Also at: Physics Department, University of Strathclyde, Glasgow, G4 0NG, U.K.
[**] Chief Technologist, EFDA-JET (Joint European Torus), Culham Science Centre, Abingdon, OX14 3DB, U.K.
[††] Mechanical Engineer, ITER (International Thermonuclear Experimental Reactor) Systems, Culham Science Centre, Abingdon, OX14 3DB, U.K.

Nomenclature

AGM = Artificial Gravity Module
D4H = Delta IV Heavy
DSV = Deep Space Vehicle
EDS = Earth Departure Stage
ILS = Inter-Lander Structure
LAS = LSM Adaptor Structure (LSM & MTS-L)
LDA = LIDS Docking Adaptor (LSM & Landers)
LDS = LIDS Docking Structure (DSV3)
LIDS = Low Impact Docking System
LSM = Lander Service Module
MAS = MTS-C Attach Structure
MCL-H = Mars Cargo Lander – Habitat Variant
MCL-R = Mars Cargo Lander – Rover Variant
MCTV = Mars Crew Transfer Vehicle
MDA = MPCV Docking Adaptor
MLTV = Mars Lander Transfer Vehicle
MOLA = Mars Orbiter Laser Altimeter
MPCV = Multi-Purpose Crew Vehicle
MPL = Mars Personnel Lander
MRA = MTS-C Rendezvous Assembly
MTS = Mars Transfer Stage used for MLTV and MCTV
MTS-C = MTS used for MCTV, with MAS & MRA added
MTS-L = MTS used for MLTV, with LAS added
SLS = Space Launch System

I. Introduction

This paper presents a conceptual Mars Exploration Vehicle (MEV) architecture, which uses a combination of Earth orbit rendezvous (EOR), Mars orbit rendezvous (MOR), and Mars surface rendezvous (MSR) to accomplish an exploration of Mars' surface with a four-person crew. Aerobraking is used in conjunction with propulsive braking for Mars orbit insertion to significantly reduce injected mass to low Earth orbit (IMLEO). The MEV architecture includes two unmanned Mars Lander Transfer Vehicles (MLTVs) and a Mars Crew Transfer Vehicle (MCTV) with a crew of four. The MLTVs and MCTV are assembled in low Earth orbit (LEO) from modules launched by four Space Launch System (SLS) and five Delta IV Heavy (D4H) rockets. The two MLTVs and the MCTV each individually escape from LEO, transit to Mars, brake into Mars orbit using propulsion and aerobraking, and rendezvous and dock in low Mars orbit (LMO). Each MLTV includes an Earth Departure stage (EDS), Mars Transfer Stage (MTS-L), Lander Service Module (LSM), and two landers: A Mars Personnel Lander (MPL) provides two-way crew transportation between LMO and the surface. Three unmanned Mars Cargo Landers (MCLs) provide one-way cargo transportation and the functionalities of habitats (MCL-H) (2) and rover (MCL-R). The landers rendezvous and assemble on the surface to form a base. The MCTV includes two EDS, two MTS-C, and the following: (1) The Multi-Purpose Crew Vehicle (MPCV) transports the crew from Earth to LEO, provides propulsion, and returns the crew to Earth after completion of the nominal mission or in abort situations. (2) Three Deep Space Vehicles, DSV1, DSV2, and DSV3, provide life support consumables, passive crew biological radiation shielding, crew habitation space, and propulsion. The DSV design was derived from the MCL-H. (3) An Artificial Gravity Module (AGM) allows the MCTV to rotate and generate artificial gravity for the crew and provides photo-voltaic power generation and deep space communications. A miniature magnetosphere (Mini-Mag), a potential key

enabler for human interplanetary exploration, is generated on the AGM by a superconducting electromagnetic coil and provides active crew biological radiation shielding. The MEV architecture is based on many existing or near-term technologies. It incorporates significant modularity and could provide an economical approach to achieve progressively more ambitious stepping stone missions along a flexible path for human solar system exploration: starting with test flights in Earth and lunar orbit and progressing through missions to near-Earth asteroids and the moons of Mars, and culminating in the Mars landing mission. The MEV architecture is based on a vehicle design to accomplish a human exploration of Near Earth Object (NEO) asteroids, the NEO Exploration Vehicle (NEV).[1]

The purposes of this paper are twofold: (1) to present an innovative vehicle architecture for human exploration of Mars, the Mars Exploration Vehicle (MEV) architecture. The MEV has key features that will be needed to keep the crew healthy and safe during a ~30 month duration round-trip mission to Mars: sufficient volume for human habitation, artificial gravity to prevent deterioration of the human body caused by prolonged periods in microgravity, and effective passive and active crew biological shielding from solar and cosmic radiation to prevent radiation sickness. The MEV design is flexible and modular, and can be used for human exploration missions to lunar orbit and NEO asteroids before being used on missions to Mars. Its use on these shorter-duration precursor missions will demonstrate key technologies for the longer duration Mars missions. (2) to present the Mini-Magnetosphere (Mini-Mag) concept for active crew biological radiation shielding.[2] The Mini-Mag could be a key enabler for human interplanetary exploration, affording the crew effective protection from the interplanetary radiation environment.

II. MEV Requirements, Architectural Considerations, Design Overview, and Flight Performance

A. MEV Mission Requirements

Reference 3 describes a human exploration mission to Phobos and Deimos for both 2033 and 2035 opportunities. It provided the requirements for velocity change (δV) and mission durations shown in Table 1. This mission outlined in this paper assumed δVs of 3,700 m/s for Trans-Mars Injection (TMI) and 2,150 m/s for Trans-Earth Injection (TEI) to cover requirements for both 2033 and 2035 opportunities. 3,700 m/s TMI was estimated to permit a 30-day earlier than optimal MLTV launch. The MEV architecture assumes both propulsive braking and aerobraking for MOI, hence the lower δV shown in Table 1 for MOI. δVs assumed for course corrections and Flight Performance Reserve (FPR) are also shown in Table 1. δV for Entry Corridor Control (ECC) burns and Mission Performance Reserve (MPR), not shown in Table 1, were assumed and shown in section IV.D, below. Reference 4 provided representative orbital alignments for a 2033 long-stay conjunction class mission shown in Fig. 1. For vehicle sizing purposes, this paper assumed a mission with a 210 day outbound transit; a 480 day stay at Mars, and a 210 day inbound transit, with the two MLTVs departing ~30 days earlier than the MCTV. MEV architectural considerations are discussed in section II.B, below, and the MEV mission is outlined in sections III and IV, below.

Table 1. Mars Mission δVs for 2033 & 2035 Opportunities.

Mars Mission Opportunity	2033	2035	MEV (Net)	MEV (Max)
Main Propulsive Burn (m/s) [1]				
Trans-Mars Injection (TMI) [2, 3]	3,520	3,620	3,700	3,774
Mars Orbit Insertion (MOI) [4, 5, 6]	1,800	1,360	800	842
Trans-Earth Injection (TEI) [7, 8]	1,620	2,150	2,150	2,219

[1] Burns include 2% Flight Performance Reserve (FPR) on δV.
[2] TMI δV estimate 3,700 m/s max. for 30 day launch window.
[3] TMI: 3,700 m/s + 2% FPR = 3,774 m/s.
[4] Aerobraking used to circularize highly elliptic capture orbit after MOI burn and compensate for ~1,000 m/s δV deficit.
[5] MOI includes Outbound Course Correction (OCC) δV.
[6] MOI: 800 m/s + 25 m/s (OCC) + 2% FPR = 842 m/s.
[7] TEI includes Inbound Course Correction (ICC) δV.
[8] TEI: 2,150 m/s + 25 m/s (ICC) + 2% FPR = 2,219 m/s.

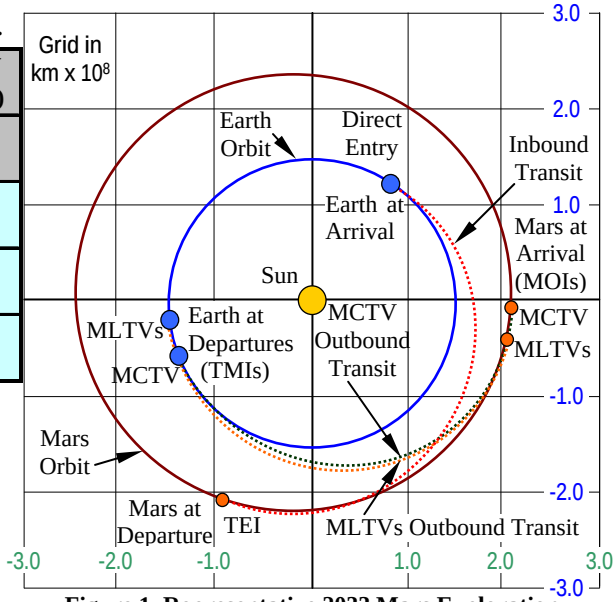

Figure 1. Representative 2033 Mars Exploration Mission Opportunity showing Orbital Alignments.

B. MEV Architectural Considerations

Many different considerations shaped the MEV architecture design:

- Provide a "minimalist" design with a crew of four, which seems to be a minimum reasonable crew size for a mission to Mars. The MPCV also will support a crew of four for deep space missions, and the Mars Personnel Lander (MPL) discussed in this paper was also designed with a maximum crew of four.
- Minimize the number of SLS launches to assemble the MEV, sizing the MEV architecture to be launched by only four SLS, the current capability of the VAB, and augmenting the SLS launches with the D4H.
- SLS assumptions: 130 metric ton (t) to 407 km (220 nmi.) circular orbit; 8.4m diameter payload shroud.
- D4H assumptions: 28t to 407 km (220 nmi.) circular orbit; 5.0m diameter payload shroud.
- Use few simple docking events to assemble the MLTV and MCTV in the low Earth parking orbit.
- Extensively use existing or near-term technology to minimize development cost and risk, such as the Centaur rocket stage, RL10-B-2 rocket engine, and the MPCV Orion Main Engine (OME) and thrusters.
- Use the existing capability of the Vehicle Assembly Building (VAB) at Kennedy Space Center (KSC) to process four SLS rockets simultaneously, and the demonstrated capability of KSC Launch Complexes 39A and 39B to have two large rockets (e.g. Space Shuttles) ready to launch almost simultaneously.
- Use launch window requirements for two MLTVs to launch 30 days before MCTV. The MEV assumes two pairs of SLS launches 30 days apart, two for the MLTVs, and two for the MCTV, to take advantage of the low-energy 2033 or 2035 launch windows. These must be supported by the five D4H launches.
- Use the existing Space Launch Complex (SLC) 37B for D4H with reasonable future launch rates of one D4H launch every 15 days. This may require that the second launch complex (SLC-37A) be refurbished.
- Set the requirement for all architectural elements to be launched to Mars during a single opportunity, and sequence the Earth departures and Mars arrivals such that two MLTVs can rendezvous with the MCTV.
- Enable all vehicles to dock together at either end to permit the MCTV to be easily reconfigured. In the case of the DSVs, two additional side docking ports are provided, in addition to forward and aft docking ports, to enable two landers each to dock to DSV1 and DSV2, and two MTS-Cs to dock to DSV3.
- The ability to rotate the MCTV to provide AG was a strong contributor to how the MCTV was designed. Strong consideration was given to balancing the vehicle in a dumbbell configuration, using roughly equal masses on both sides of the vehicle during all mission phases, to enable sufficient AG rotation.
- The physical layout and mass of the heavy MiniMag electromagnetic coil and associated equipment including structural supports, thermal isolators, cryostat, cryocoolers, and batteries also drove the design.

C. MEV Design Overview

The Mars Exploration Vehicle Architecture (MEV) is modular and assembled in low Earth orbit (LEO) from subassemblies launched by the SLS and D4H. It is comprised of two types of vehicles: (1) the Mars Lander Transfer Vehicle. Two MLTVs each transport two Mars landers on a one-way trip from the Earth parking orbit to the Mars parking orbit; and (2) the Mars Crew Transfer Vehicle. The MCTV transports the four person crew on a round trip between Earth and Mars, from the Earth parking orbit to the Mars parking orbit, and back to a direct Earth entry.

1. Mars Lander Transfer Vehicle (MLTV)

The unmanned MLTV is shown in Fig. 2. The MLTV is assembled in a 407 km (220 nmi.) circular parking orbit from two subassemblies launched by one SLS booster and one D4H booster. It is composed of the following major components: an Earth Departure Stage (EDS) utilizing cryogenic propellants, a Centaur-Derived Mars Transfer Stage (MTS) utilizing cryogenic propellants, two Mars landers, an MCL-H and MPL/MCL-R, and a Lander Service Module (LSM) utilizing storable hypergolic propellants. MCL and MPL lander designs are discussed in sections IV.C and V.D. MTS, EDS, and LSM designs are discussed in sections V.A, V.B, and V.C, respectively.

2. Mars Crew Transfer Vehicle (MCTV)

The MCTV, with a crew of four, is shown in Fig. 3. The MCTV is assembled in the 407 km (220 nmi.) parking orbit from five subassemblies launched by two SLS and three D4H. It is composed of the following major components: two EDS, two MTS, an MPCV utilizing storable hypergolic propellants, three Deep Space Vehicles, DSV1, DSV2, and DSV3, utilizing storable hypergolic propellants, and an Artificial Gravity Module (AGM).

The MPCV transports the crew from earth to LEO. It is launched separately and docks with the other MCTV subassemblies already in LEO. The MPCV also provides for return of the crew to earth after successful completion of the mission or in abort situations. MPCV design parameters were taken from recent NASA publications (see Ref. 1) on its predecessor, the Orion Crew Exploration Vehicle and were used in this paper without any modifications.

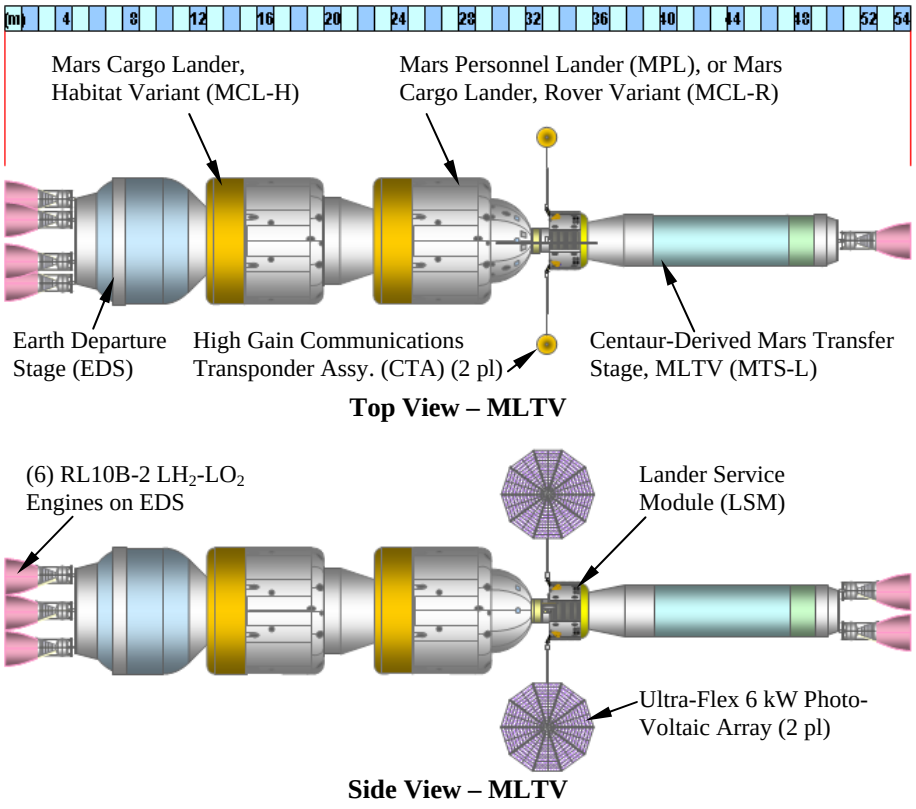

Figure 2. Configuration Top and Side Views – Mars Lander Transfer Vehicle (MLTV).

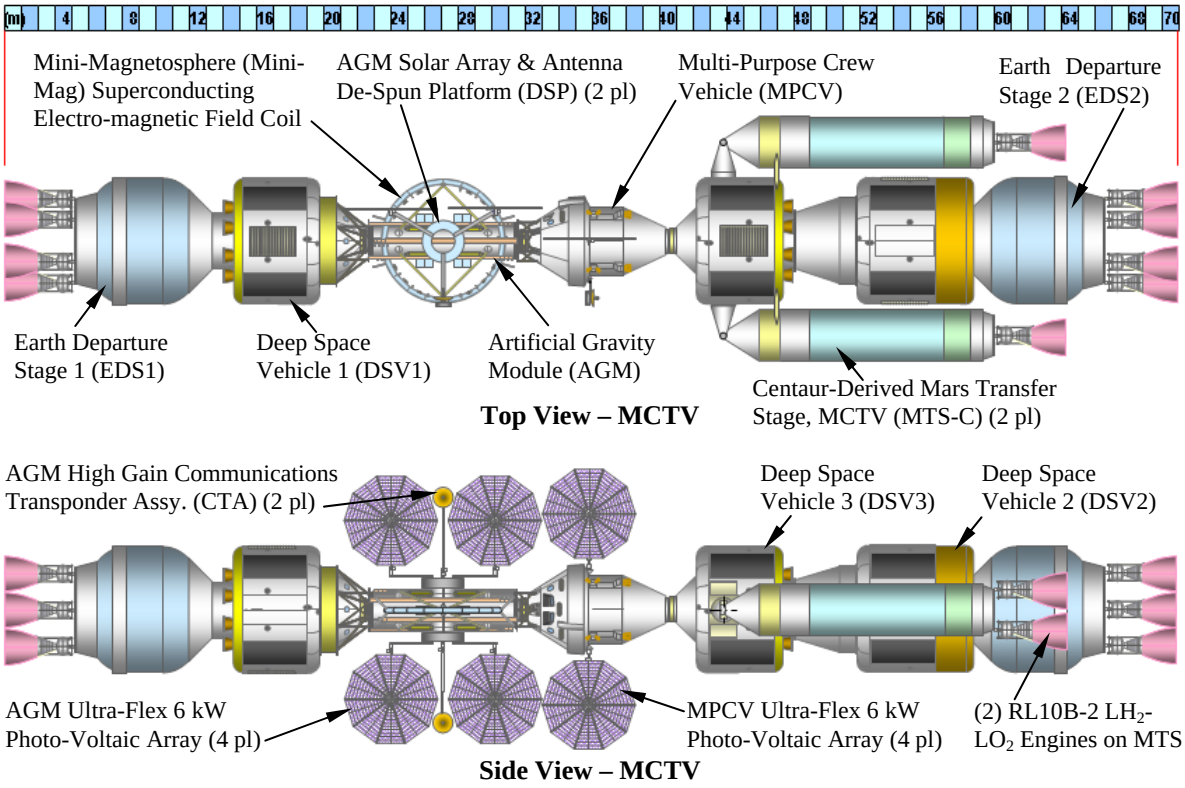

Figure 3. Configuration Top and Side Views – Mars Crew Transfer Vehicle (MCTV).

The DSV1, DSV2, and DSV3 provide supplemental propulsion, habitation volume, life support consumables, and passive biological radiation shielding for four crewmembers on long-duration deep space missions. DSV1 and DSV2 provide the crew living quarters during the bulk of the mission. The DSV design is derived from the common modular landers used in the Spaceship Discovery vehicle architecture for human exploration of the solar system.[5] The DSV is a modification of the Spaceship Discovery LM3 autonomous cargo lander, habitat variant (renamed MCL-H in this paper).[6] The DSV design is discussed below in section V.E.1, Design of Deep Space Vehicle (DSV).

The AGM links the two sides of the MCTV, the DSV2/DSV1 and MPCV/DSV3, together mechanically and electrically using telescoping artificial gravity (AG) rails. The AG rails can extend to separate the DSV2/DSV1 and MPCV/DSV3 from the AGM to get long radius arms for AG rotation of the MCTV, providing a nominal 0.379 Earth g's (Mars surface equivalent) of artificial gravity generated by centrifugal force in the DSV2 mid-level crew cabin during outbound transit, Mars orbit phase, and inbound transit. The MCTV AG concept is described in detail in Ref. 1. It has the flexibility to vary the length of the radius arms, depending on the relative vehicle component masses which vary throughout the mission. The MCTV is spun-up and spun-down using DSV2 and DSV3 thrusters during the outbound transit and Mars orbit phase, and DSV2 and MPCV thrusters during the inbound transit. The MCTV rotates in a plane parallel to the plane of the ecliptic to facilitate solar array Sun tracking and antenna Earth tracking. The AGM provides a tunnel for pressurized crew access between the MPCV and DSV1 when the MCTV is not rotating (zero-g) and MPCV and DSV1 have been retracted and docked to the AGM. The AGM also provides photo-voltaic power generation, deep space communications, and the Mini-Mag active biological radiation shield. The Mini-Mag is generated by a powerful superconducting electromagnetic coil in the AGM. Figure 4 shows the general form of the magnetic lines of force generated by the Mini-Mag around the MCTV interacting with the solar wind. The Mini-Mag theory of operation was described in detail in Ref. 1. The design of the AGM is discussed below in section V.F, and the design of the Mini-Mag electromagnetic coil system is discussed below in section VI.

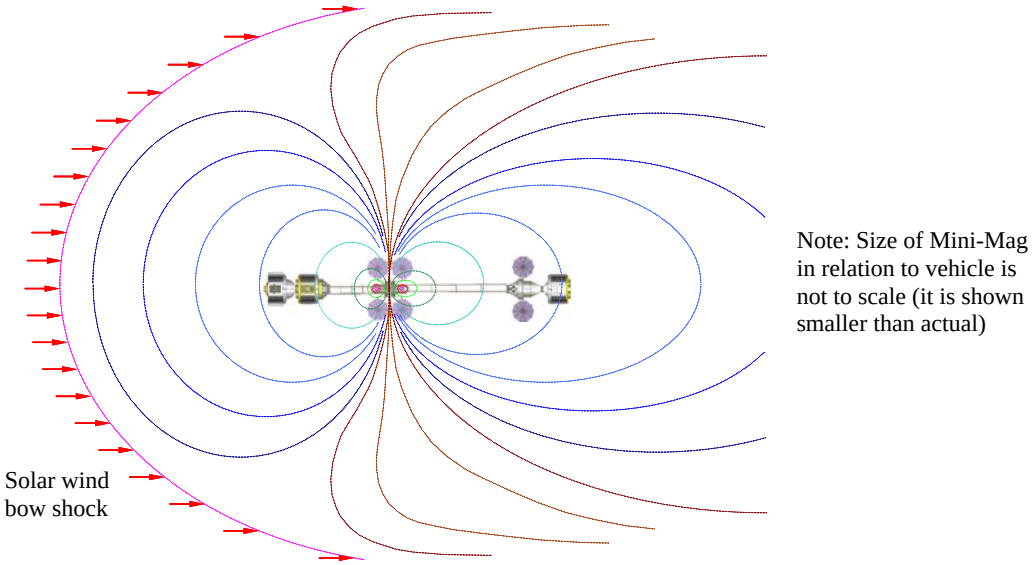

Figure 4. The Mini-Magnetosphere Shield – General Form of Magnetic Lines of Force around Vehicle in Solar Wind.

D. MEV Mass Estimation and Flight Performance Calculations

Masses for MEV system components were scaled using data for existing spaceflight hardware where possible, such as the RL10-B-2 engine, MPCV Orion Main Engine (OME), and hardware that has been flown on the Space Shuttle or Apollo. Test data from developmental hardware such as the MPCV Ultra-Flex solar arrays provided additional anchor points. Also included was commercial off the shelf spaceflight hardware such as satellite apogee motors and thrusters, and mass data from pertinent space vehicle studies such as the Altair lunar lander. Structural analyses were performed for major MEV components, for various important load cases, to validate conceptual design mass scaling laws that were input to the MEV mathematical model discussed below. Tables 2, 3, 4, and 5 provide summaries of MEV component masses. Initial masses are shown for the EDS, MTS, LSM, AGM, MPCV, DSV1, DSV2, and DSV3. Future work will continue to refine MEV component mass estimates. Table 6 provides assumed Life Support System (LSS) consumables usage rates and masses that were input to performance analyses.

The SLS is assumed to be able to lift 130 metric tons (t) of payload into a circular, 407 km (220 nautical mile) altitude parking orbit for vehicle assembly. The D4H is assumed to be able to lift 28t into the same circular, 407 km (220 nmi.) altitude parking orbit. Burn δV assumptions: 3700 m/s for the Trans-Mars Injection (TMI) burns, 25 m/s for outbound course correction (OCC) burns, 800 m/s for the Mars Orbit Insertion (MOI) burn, with aerobraking making up the δV deficit, 2,150 m/s for the Trans-Earth Injection (TEI) burn, 25 m/s for inbound course correction (ICC) burns, 25 m/s for the Entry Corridor Control (ECC) burn, 30 m/s for mission performance reserve (MPR), and 2% flight performance reserve (FPR) (on all burns). For this analysis, δV for OCC was included in the MOI burn, δV for ICC was included in the TMI burn, and δV for Mission Performance Reserve (MPR) was included in the ECC burn. A mathematical model was used to size the MLTV and estimate its flight performance: (1) the EDS had variable inert and propellant masses; (2) the MTS-L had variable inert and propellant masses; (3) the LSM had variable inert and propellant masses; and (4) the landers were treated as fixed payloads. A second mathematical model was used to size the MCTV and estimate its flight performance: (1) the EDS and MTS-L had variable inert and propellant masses, and were iterated with the MLTV to derive common EDS and MTS designs; (2) the MPCV had fixed inert and variable propellant masses, with fixed initial and final payload masses. Its mass of consumables was held fixed as a mission reserve; (3) AGM mass was fixed throughout the mission; (4) DSV1, DSV2, and DSV3 inert, propellant, consumables, and payload masses varied throughout the mission; and (5) as DSV propellant mass was increased to achieve δV targets, propellant and pressurant tank sizes and masses, and backup structure mass were increased using scaling laws. Future work will refine the MLTV and MCTV flight performance estimates.

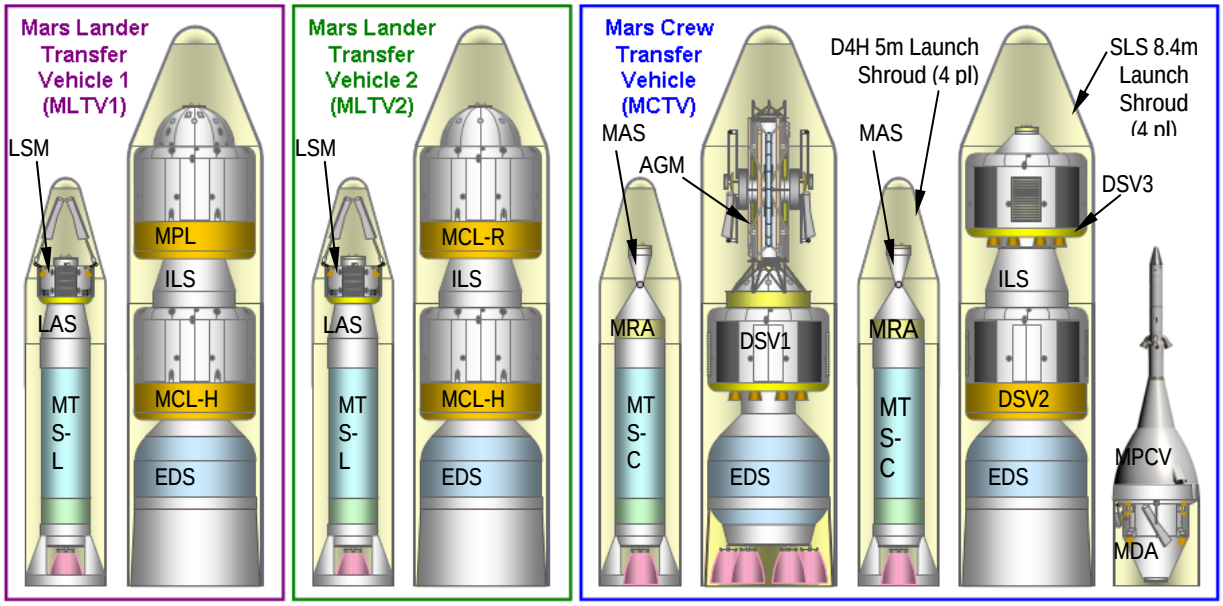

Figure 5. Mars Exploration Vehicle Architecture (MEV) Launch Configurations.

Table 2. Mars Exploration Vehicle Architecture (MEV) Launch Masses.

Mass, Metric Tons (t)	Vehicle Designator	MLTV1		MLTV2		MCTV				
	Launch Vehicle	D4H1	SLS1	D4H2	SLS2	D4H3	SLS3	D4H4	SLS4	D4H5
Earth Departure Stage (EDS)	Usable Propellant		77.40		77.40		8.60		8.60	
	Inert & Residuals		8.60		8.60		77.40		77.40	
	Total Mass		86.00		86.00		86.00		86.00	
Mars Transfer Stage (MTS)	Usable Propellant	20.92		20.92		24.30		24.30		
	Inert & Residuals	2.70		2.70		2.70		2.70		
	Total Mass	23.62		23.62		27.00		27.00		
Remainder of Mission Payload		4.38	44.00	4.38	44.00	1.00	42.47	1.00	38.35	23.04
Injected Mass to LEO (IMLEO)	Total for Launch	28.00	130.00	28.00	130.00	28.00	128.47	28.00	124.35	23.04
	Total for Vehicle	158.00		158.00		331.87				
	Total for Mission	647.87								

.

Table 3. AGM Initial Mass Breakdown.

Artificial Gravity Module (AGM)	Mass (kg)
Structure and Subsystems	
Pressurized Structural Tube (PST)	650
Space Frames (2)	240
(2) Despun Platforms	120
(2) Passive LIDS	100
AG Extension Rails (8 sets)	640
DC Power Electronics	73
(4) Solar Arrays	128
(2) Antennas & Comm Equip.	40
Dry Mass Margin (15%)	299
Subtotal, Structures & Subsys	2,289
Subtotal, Mini-Mag System [1]	3,185
Total Mass, AGM	5,474

[1] See table 10 for MiniMag System mass breakdown.

Table 4. MPCV Initial Mass Breakdown.

Multi-Purpose Crew Vehicle (MPCV)	Mass (kg)
Initial Payload: (4) Crewmembers & Equip.	
(1) Crew Member	80
(1) Spacesuit	35
(1) [1] ELSS Unit	5
(1) [2] EVA PLSS Backpack	45
(1) Crew Member and Equipment	165
Subtotal, Initial P/L: (4) Crew & Equip.	660
Subtotal Non-Propellant Mass	13,475
Subtotal Propellant Mass	7,907
Total Mass	22,042

[1] Emergency Life Support System.
[2] Extra Vehicular Activity, Personal Life Support Sys.

Table 5. DSV1, DSV2, & DSV3 Initial Mass Breakdowns.

Deep Space Vehicle (DSV)	DSV1	DSV2	DSV3
DSV Habitat Stage (HS)			**(N/A)**
Subtotal, Outbound Payload [1]	0	0	
Structure, Insulation, TCS	1,807	1,807	
Subsystems	384	384	
RCS Dry Mass	0	50	
Dry Mass Margin (15%)	329	336	
Subtotal, HS Inert Mass	2,520	2,577	
Subtotal, HS LSS Consumables [2]	7,234	7,234	
Subtotal, HS RCS Propellant	0	250	
Total Mass, Habitat Stage	9,754	10,061	0
DSV Propulsion Stage (PS)			
[3] Subtotal, Outbound Payload	400	800	500
Structure, Insulation, and TCS	520	520	520
Propellant Tanks	970	40	566
Fixed and Inflatable Heatshield	0	750	0
Subsystems	184	184	184
(8) Main Engines & Installation	487	0	487
RCS System Dry Mass	99	99	99
Dry Mass Margin (15%)	339	239	278
Subtotal, PS Inert Mass	2,599	1,832	2,135
Subtotal, RCS Propellant Mass	509	998	996
Subtotal, PS LSS Consumables [2]	0	6,883	0
Subtotal, PS Main Propellant	23,738	0	13,144
Total Mass, Propulsion Stage	27,246	10,513	16,775
Total Mass, DSV	37,000	20,575	16,775

[1] (4) Crewmembers with space suits, ELSS, and PLSS launch in MPCV and transfer to DSV1/DSV2 after TMI burns completed.
[2] See Table 6 for breakdown of life support consumables masses.
[3] DSV1: Airlock; DSV2: Airlock, (2) Manned Maneuvering Units (MMUs) and propellant; DSV3: LIDS Docking Adaptor (LDA).

Table 6. LSS Consumables Endurance for MEV with 4 Person Crew.

Mission Phase	OTO	LMO	ITO	Reserve	Total
Consumables Location	**DSV2-HS**	**DSV2-HS**	**DSV2-HS**	**MPCV**	**All**
Duration (days)	210	480	210	21	921
Duration (months)	7	16	7	0.7	30.7
Endurance (man-day)	840	1920	840	84	3684
Consumable Consumption Rates (kg/m-day)					
Breathing Oxygen	1.300	1.300	1.300		
Water Before Recovery [1]	5.200	2.900	5.200		
Water After Recovery [1]	0.780	0.435	0.780		
Food	1.850	1.850	1.850		
LSS Consumable Masses (kg)					
Breathing Oxygen	1,092	2,496	1,092		
Water	4,368	835	4,368		
Dry Food	1,554	3,552	1,554		
Nitrogen [2]	220	0	220		
Subtotal Consumables Masses	7,234	6,883	7,234		
Total Consumables Mass			21,351		

[1] Fraction of wastewater recovered = 0.850.
[2] For airlock/cabin atmosphere reconstitution and MMU recharge.

III. MLTV Design, Mission Description, and Flight Performance

A. MLTV Design Overview and Assembly in LEO

Each MLTV transports two Mars landers to low Mars orbit (LMO). MLTV1 transports the MCL-H and MPL. MLTV2 transports a second MCL-H and the MCL-R. Each lander pair is mated to an inter-lander structure (ILS) that joins the two landers. The lower lander in the stacked pair, the MCL-H, also carries a LIDS Docking Adaptor (LDA) that provides an active LIDS assembly on each side, to mate with the passive LIDS on the MCL-H and the MCTV side docking hatches. The second LDA (to provide active LIDS capability to the upper lander in the stacked pair, the MPL/MCL-R) is transported to the MLTV by the LSM/MTS-L stack which is launched by the D4H. The two-lander assembly is mated to an EDS, and the entire MPL/MCL-H/EDS (or MCL-R/MCL-H/EDS) stack is enclosed in the NASA Space Launch System (SLS) heavy lift launch vehicle payload shroud. The MCTV launch concept is as follows: the two D4H rockets used for MLTV1 and MLTV2 are launched 30 days and 15 days, respectively, before the SLS launch date. The two LSM/MTS-L stacks station keep and wait for the SLS launches. The MTS is well insulated and experiences minimal boil-off of propellant while loitering 30 or 15 days in LEO as described in section V.A. below. The two SLS rockets are then launched from pads 39A and 39B on the same day, to minimize boil-off of propellant from the EDS before TMI. The SLS launches target the positions of the two LSM/MTS stacks launched previously. The LSM/MTS stack performs the active role in the rendezvous and docking phase. All four launchers inject their payloads into a 407 km (220 nautical mile) circular parking orbit. Figure 6a-b shows the LSM/MTS stack rendezvous and docking with the MPL/MCL-H/EDS stack to complete MCTV1.

B. MLTV Mission Description and Flight Performance, TMI through Rendezvous with MCTV

Figures 6c-l outline the MLTV mission from TMI burns through Rendezvous w/ MCTV in the Mars parking orbit. The TMI is a two-stage burn, shown in Figs. 6c-e, which uses all of the propellant in the EDS, and approximately half of the propellant in the MTS. During the ~210 day outbound transit from the Earth parking orbit to the Mars parking orbit shown in Fig. 6f, the MPL/MCL landers will be kept in a hibernation mode to conserve power. The MLTV lander base is covered in reflective foil and kept pointed at the sun to shadow the MTS propellant tanks. The MOI burn, shown in Figs. 6g-h, uses approximately 1,000 m/s less dV than needed for insertion into a circular orbit. Aerobraking is used to circularize the orbit as shown in Figs. 6i-l and 7. References 7-10 provide details of aerobraking utilized by recent unmanned scientific spacecraft to attain circular orbit around Mars with δV deficits comparable to the MLTV. The MCTV discussed in section IV, below, will also use this technique. Future work will provide the timeline for aerobraking and additional details. After completion of aerobraking, the MLTV enters into a 500 km altitude circular parking orbit and waits for the MCTV, for rendezvous and transfer of the landers to the MCTV. Table 7 provides a summary of MLTV flight performance data.

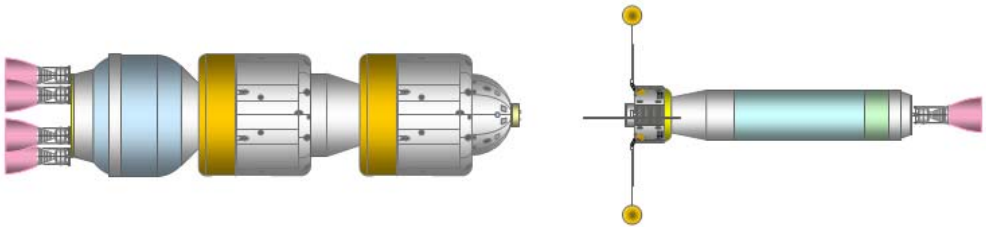

a. MLTV LEO Assembly – Rendezvous of LSM/MTS Stack with MCL/MCL-H/EDS Stack.

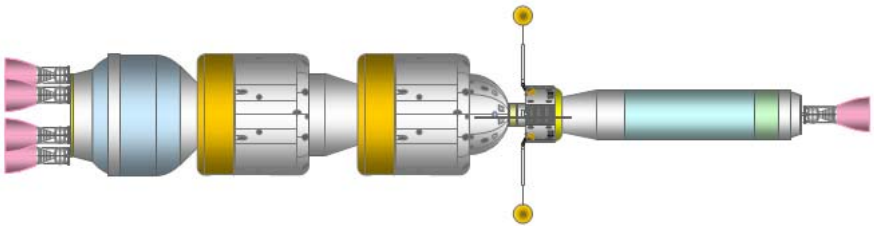

b. MLTV LEO Assembly – Docking of LSM/MTS Stack w/ MCL/MCL-H/EDS Stack; Assembly Complete.

Figure 6. Mission Description – MLTV Assembly through Rendezvous w/ MCTV.

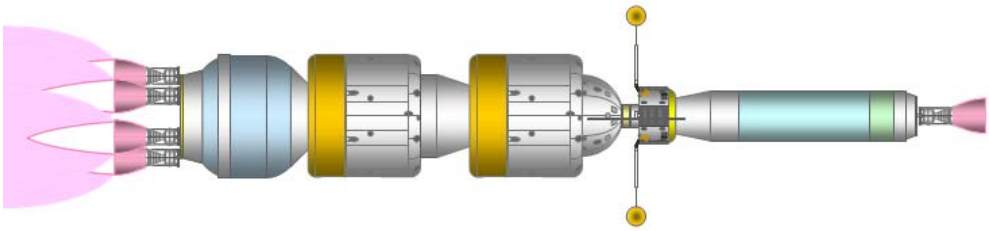

c. Earth Departure – MCTV in LEO; Trans-Mars Injection (TMI) Burn A using EDS.

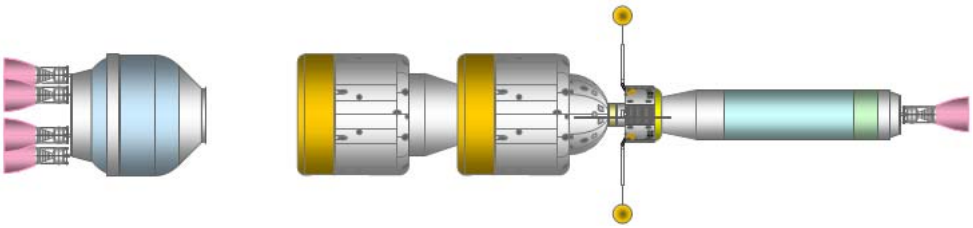

d. Earth Departure – EDS Jettisoned after TMI Burn A.

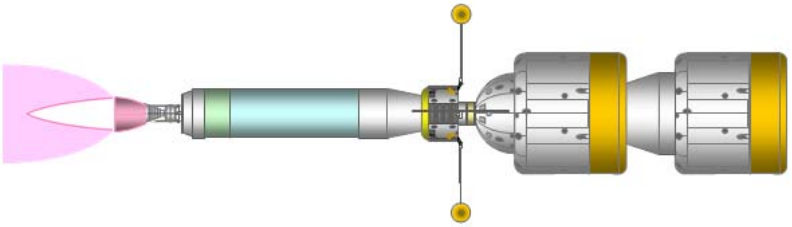

e. Earth Departure – MCTV Rotated 180 degrees; TMI Burn B using Mars Transfer Stage (MTS).

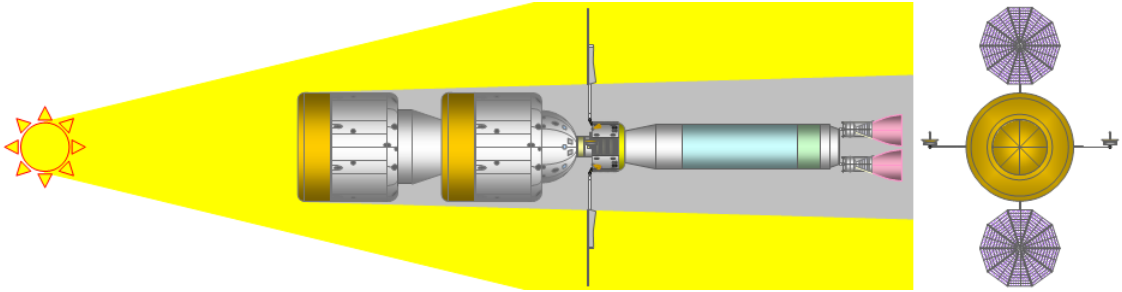

f. Outbound Transit – MCTV Points Lander Base Towards Sun to Shadow MTS Propellant Tanks.

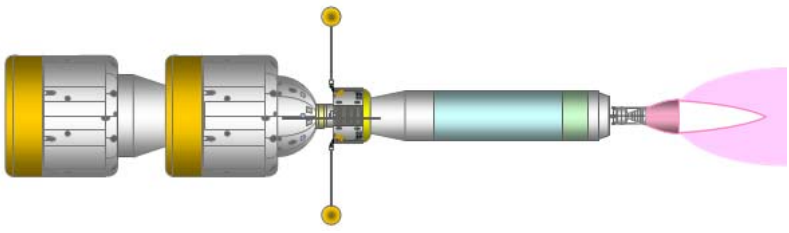

g. Mars Capture – Mars Orbit Insertion (MOI) Burn Performed by MTS.

Figure 6. Mission Description, Continued – MLTV Assembly through Rendezvous w/ MCTV.

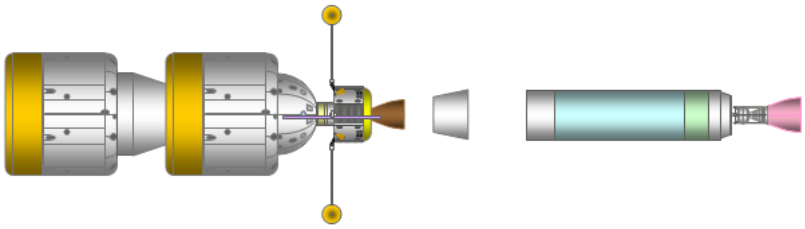

h. Mars Capture – MTS and Lander Service Module (LSM) Adaptor Structure Jettisoned after MOI Burn.

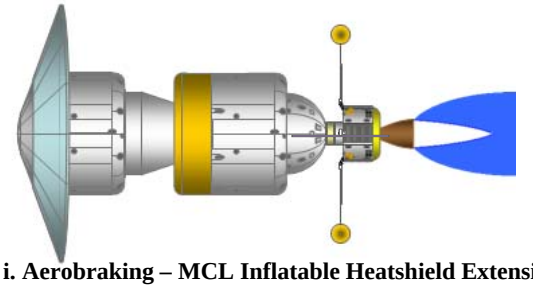

i. Aerobraking – MCL Inflatable Heatshield Extension Deployed; LSM "Walk-In" Burn to Start Aerobraking.

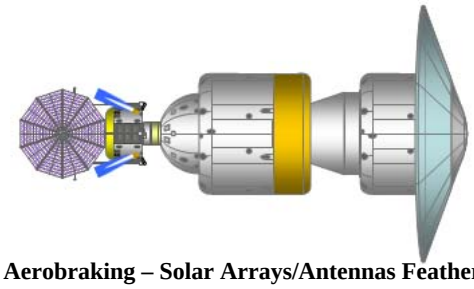

j. Aerobraking – Solar Arrays/Antennas Feathered; LSM "Trim" Burn to Control Periapsis & Density.

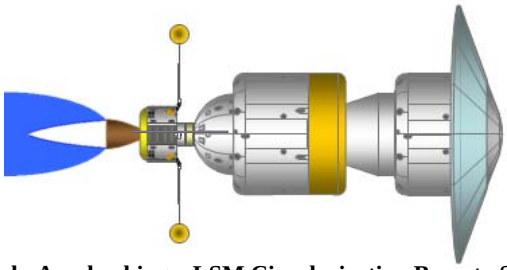

k. Aerobraking – LSM Circularization Burn to Stop Aerobraking/Raise Periapsis to Parking Orbit Altitude.

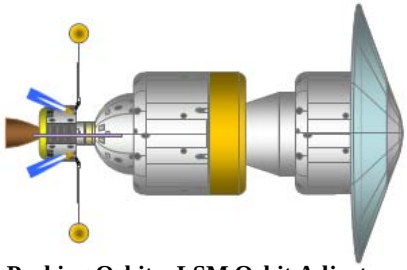

l. Mars Parking Orbit – LSM Orbit Adjustment Burn for MLTV Rendezvous with MCTV.

Figure 6. Mission Description, Continued – MLTV Assembly through Rendezvous w/ MCTV.

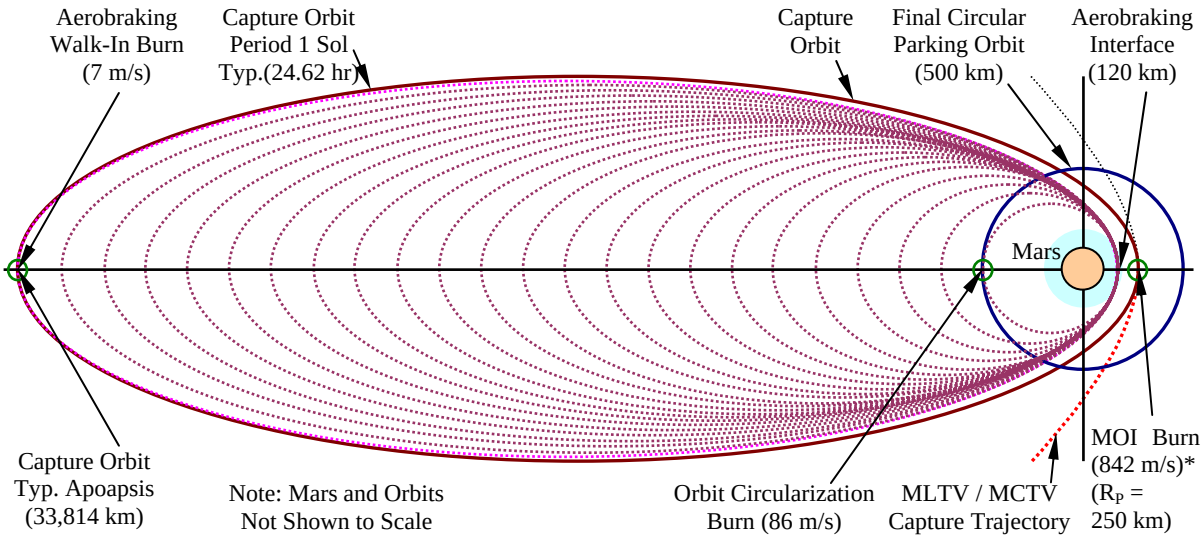

* Includes 25 m/s for Outbound Course Corrections plus 2% FPR

Figure 7. MLTV / MCTV Propulsive Capture and Aerobraking into Final Parking Orbit.

Table 7. MLTV Performance for TMI, MOI, and Aerobraking (A/B) Burns.

MLTV Mass (kg)	TMI Burn A	TMI Burn B	MOI Burn	A/B Burns
Items Launched by SLS1				
MPL Inert and Propellant	21,000	21,000	21,000	21,000
Inter-Lander Structure (ILS)	1,000	1,000	1,000	1,000
LIDS Docking Adaptor (LDA)	500	500	500	500
MCL-H Inert and Propellant	21,500	21,500	21,500	21,500
Lander Payload Total Mass	44,000	44,000	44,000	44,000
EDS1 Non-Propellant	8,600	Jettisoned		
EDS1 Usable Propellant [2]	77,400			
EDS1 Total Mass	86,000			
Total Mass	130,000	44,000	44,000	44,000
Items Launched by D4H1				
LIDS Docking Adaptor (LDA)	500	500	500	500
LSM1 Non-Propellant	1,282	1,282	1,282	1,282
LSM1 Usable Propellant [1, 2]	1,883	1,883	1,883	1,883
LSM1 Total Mass	3,165	3,165	3,165	3,165
LSM Adaptor Structure (LAS)	500	500	500	Jettisoned
MTS-L1 Non-Propellant	2,700	2,700	2,700	Jettisoned
MTS-L1 Usable Propellant [2, 3]	20,921	20,921	10,284	
MTS-L1 Total Mass	23,621	23,621	12,984	
Total Mass	27,786	27,786	17,149	3,665
Total Vehicle				
MLTV Stack Initial Mass	157,786	71,786	61,149	47,665
MLTV Stack Final Mass	80,386	61,689	50,865	45,782
Propellant Mass Consumed	77,400	10,097	10,284	1,883
Velocity Change (m/s)				
Burn Net δV	3,082	693		
Total δV TMI [4]		3,775		
Total δV MOI [4, 5]			842	
Total δV Aerobraking Phase [4]				129
Acceleration (m/s^2 or g's)				
Initial Acceleration (m/s^2)	4.191	3.071	3.605	0.701
Initial Acceleration (g_{0Earth})	0.427	0.313	0.367	0.071
Final Acceleration (m/s^2)	8.226	3.573	4.333	0.729
Final Acceleration (g_{0Earth})	0.838	0.364	0.441	0.074

[1] 214 kg propellant used (or dumped) by LSM for MTS-L rendezvous & docking w/ MLTV prior to TMI.
[2] Usable propellant masses exclude residuals.
[3] 536 kg of propellant lost to boiloff prior to MOI by MTS-L.
[4] Includes 2% Flight Performance Reserve. [5] Includes 25 m/s for OTO course correction burns.

IV. MCTV Design, Mission Description, and Flight Performance

A. MCTV Design Overview and Assembly in LEO

The MCTV is assembled in orbit from five subassemblies launched by two SLS and three D4H boosters. The assembly sequence, shown in Figs. 8a-d, is simple and direct. The first SLS launch delivers the AGM/DSV1/EDS1 stack. The second SLS launch delivers the DSV3/DSV2/EDS2 stack, with an ILS joining the DSV2 and DSV3. Two D4H launches deliver a pair of MTS-C, each with an MTS-C Rendezvous Assembly (MRA) and an MTS-C Attach Structure (MAS). The third D4H delivers the crew in the MPCV. The MPCV carries an aft-mounted MPCV Docking Adaptor (MDA) which permits the MPCV to dock with vehicles at its aft end as well as its forward end. The two D4H rockets carrying the MAS/MRA/MTS-C stacks are launched 30 days and 15 days, respectively, before the SLS launch date. The two MAS/MRA/MTS-C stacks station keep and wait for the SLS launches. The MTS-C is

well insulated and experiences minimal boil-off of propellant while loitering 30 or 15 days in LEO as described in section V.A. below. The two SLS rockets, with the AGM/DSV1/EDS1 and DSV3/DSV2/EDS2 stacks are then launched from pads 39A and 39B on the same day, to minimize boil-off of propellant from the EDS before TMI. The fifth and final launch, of a D4H with the MPCV/MDA, launches on the same day as the two SLS. The two SLS launches and final D4H launch target the positions of the two MTS-C stacks launched previously. All five launchers inject their payloads into a 407 km (220 nmi) altitude circular parking orbit. The MPCV/MDA stack docks with the AGM/DSV1/EDS1. The DSV3/DSV2/EDS2 stack then docks to the MPCV/MDA aft docking location. Lastly the two MAS/MRA/MTS-C stacks dock to the side docking locations on the DSV3, and the twin boosters are rotated 90 degrees to be parallel to the vehicle long axis, and locked in place. AGM solar arrays deploy to provide electrical power and communications transponder assemblies deploy to provide high gain command/telemetry. The MCTV is now complete and ready for TMI. The MCTV is designed to perform its TMI 30 days after TMI of the two MLTVs.

B. MCTV Mission Description & Flight Performance, TMI through Lander Docking in LMO

Figures 9 and 10a-e describe the TMI sequence for the MCTV. TMI is performed using three sequential burns to provide sufficient δV. TMI burn A uses EDS1. This burn puts the MCTV in a highly elliptical escape orbit as shown in Fig. 9 and 10a-b. TMI burn B is performed by EDS2 at the periapsis of the escape orbit, and TMI burn C is performed by the two MTS-Ls, immediately following the EDS2 burn, as shown in Figs. 9 and 10c-e. After completion of TMI, the DSV2 will relocate from DSV3 to DSV1 as shown in Figs. 10f-h. This will provide the four-person crew with 24.3m^3 of habitable volume per person, using the combined habitation volume of DSV1 and DSV2. At this point, he crew will transfer from the MPCV to DSV1 and DSV2 through the AGM tunnel. The DSV1 and DSV2 crew cabin shield tanks will be filled with water to provide 5 gm/cm^2 of passive radiation shielding. DSV1 and MPCV undock from the AGM and the AGM artificial gravity (AG) rails extend. The Mini-Mag electro-magnetic coil is energized, taking about 4 hours to fully charge from the solar arrays to produce the active radiation shield. Li-ion batteries are provided to store coil current when necessary to de-energize the coil during the mission. The MCTV is spun-up to provide 0.378 Earth g's of AG (Mars surface equivalent) in DSV2: AG rails fully extend on both sides of the AGM to maximize thruster moment arms. Two thruster pairs, one on DSV2, and one on DSV3, fire normal to the vehicle long axis in opposite directions and produce a couple around the vehicle center of mass (CM). When rotation rate is sufficient, the AG rails are driven in on both sides of the vehicle to achieve the desired rotation rate and place the CM/center of rotation at the AGM center as shown in Fig. 10i. The sequence of events to spin-down the vehicle is the opposite of spin-up. A total of four spin-up/spin-down cycles have been allocated for the outbound transit, including three course corrections, and sufficient RCS propellant mass (1,160 kg) has been reserved for this purpose. As in case of the MLTVs, the MOI burn, shown in Figs. 10j-k, uses approximately 1,000 m/s less dV than needed for insertion into a circular orbit. Aerobraking, shown in Figs. 10l-o, is used to circularize the orbit. Figures 10p-s describe the rendezvous of the two MLTVs with the MCTV and the transfer of landers to the MCTV. Table 8 provides a summary of MCTV flight performance data for TMI, MOI, and aerobraking burns.

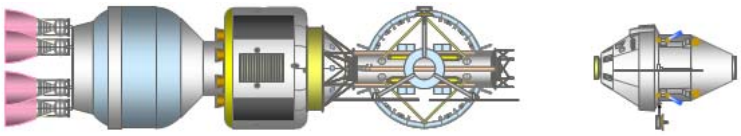

a. MCTV LEO Assembly – Rendezvous & Docking of MPCV with AGM/DSV1/EDS1 Stack.

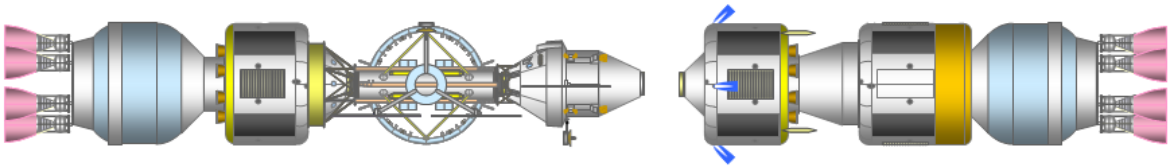

b. MCTV LEO Assembly – Rendezvous/Docking of DSV3/DSV2/EDS2 Stack w/ MPCV/AGM/DSV1/EDS1 Stack.

Figure 8. Mars Crew Transfer Vehicle (MCTV) Assembly in LEO.

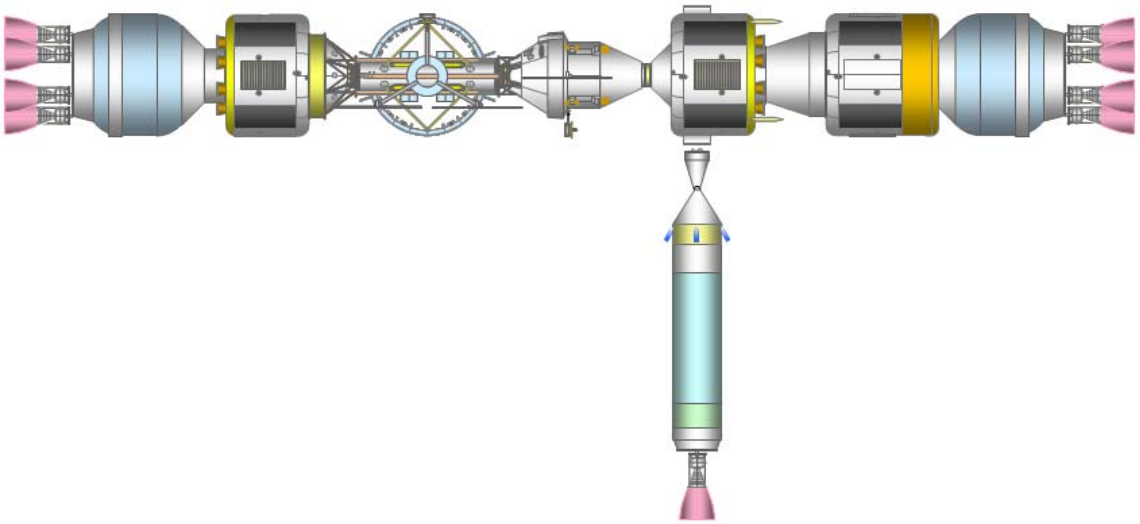

c. MCTV LEO Assembly – Rendezvous & Docking of (1 of 2) MTS w/ Assembled MCTV Components.

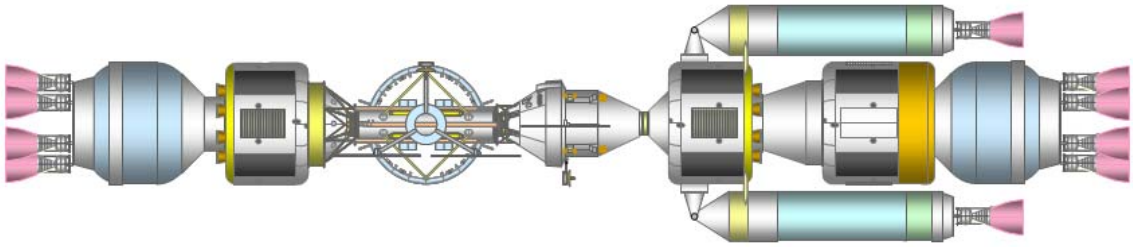

d. MCTV LEO Assembly – (2) MTS Rotated 90 Degrees and Locked to DSV3; Assembly Complete.

Figure 8. Mars Crew Transfer Vehicle (MCTV) Assembly in LEO. Continued.

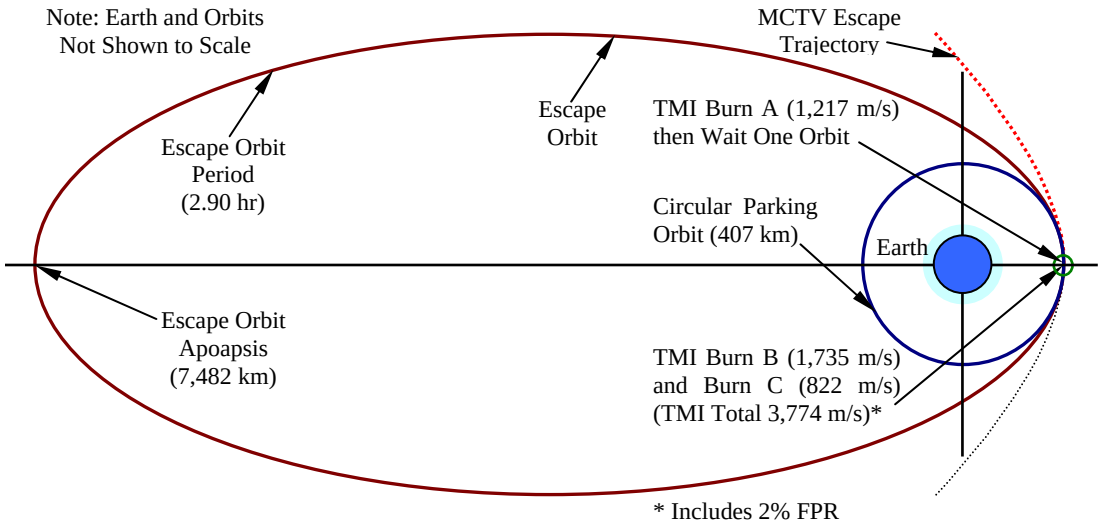

Figure 9. MCTV TMI Burn A, Escape Orbit, and TMI Burns B and C, and Earth Escape Trajectory.

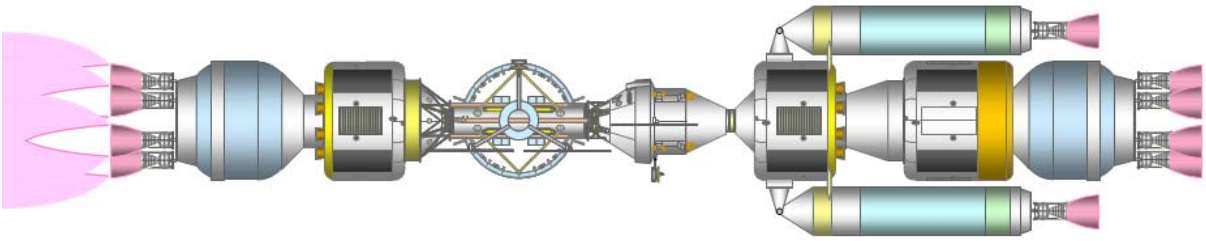

a. Earth Departure – MCTV in LEO; Trans-Mars Injection (TMI) Burn A using EDS1.

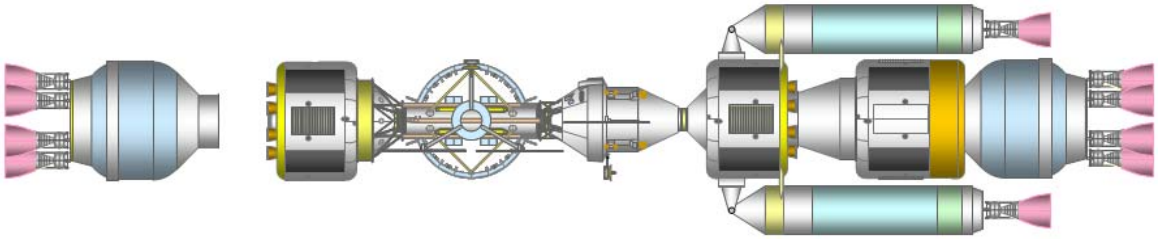

b. Earth Departure – MCTV in Escape Orbit; EDS1 Jettisoned after TMI Burn A.

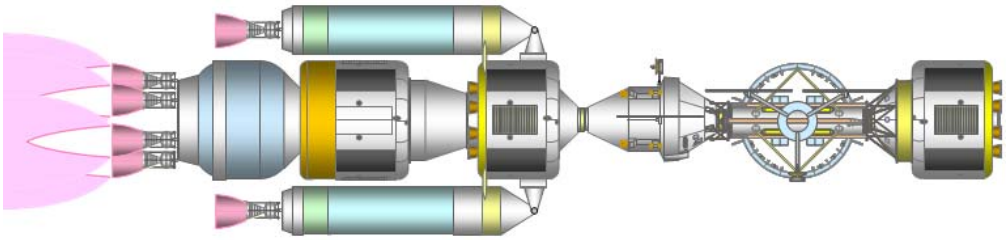

c. Earth Departure – MCTV in Escape Orbit; Vehicle Rotated 180 Degrees; TMI Burn B using EDS2.

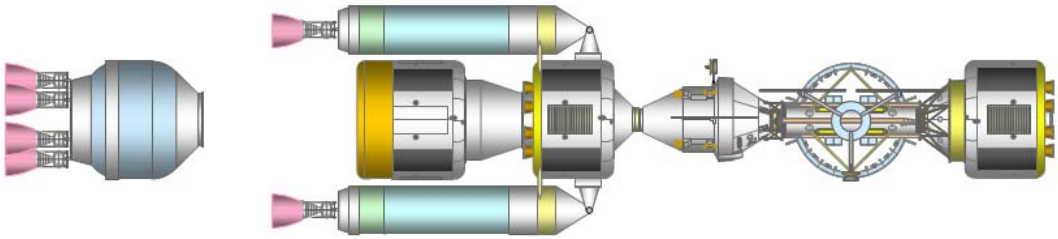

d. Earth Departure – MCTV in Escape Orbit; EDS2 Jettisoned after TMI Burn B.

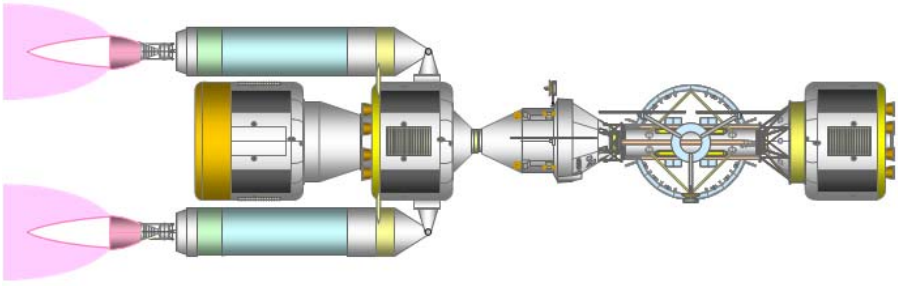

e. Earth Departure – MCTV in Escape Orbit; TMI Burn C using (2) Mars Transfer Stage (MTS-C).

Figure 10. Mission Description – TMI through Lander Docking to MCTV.

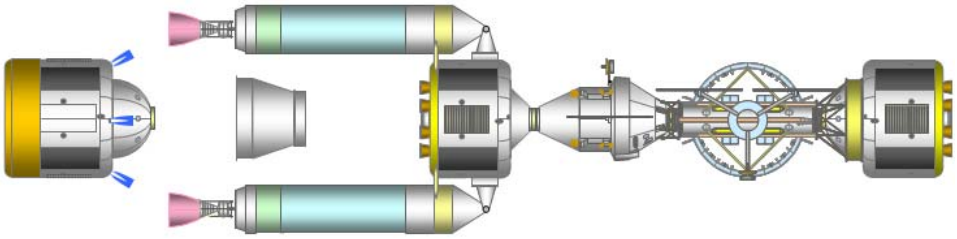

f. Outbound Transit – DSV2 Separates from Stack; Inter-Vehicle Structure Jettisoned.

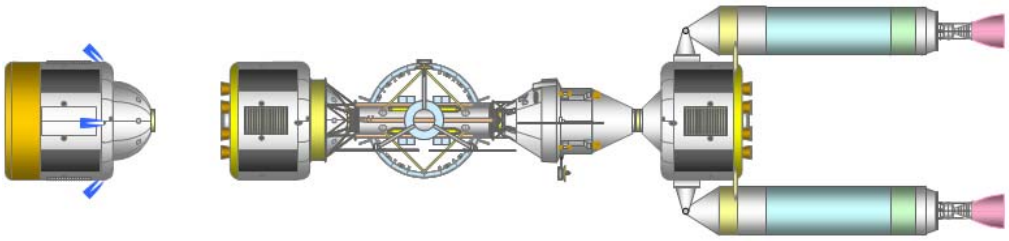

g. Outbound Transit – Vehicle Rotated 180 Degrees; DSV2 Maneuvers to Aft Docking Hatch of DSV1.

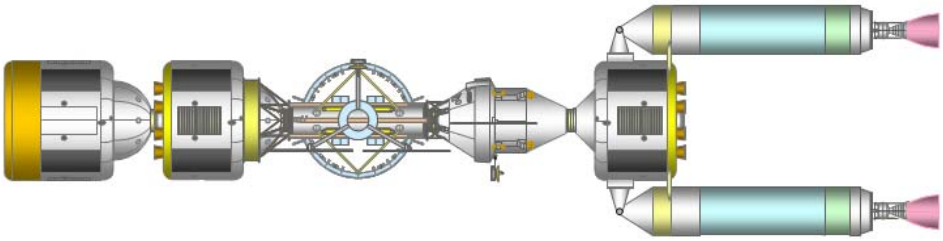

h. Outbound Transit – DSV2 Docks to Aft Docking Hatch of DSV1.

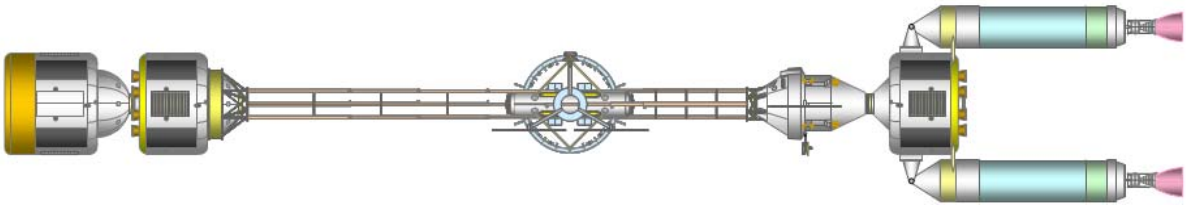

i. Outbound Transit – DSV1 & MPCV Undock from AGM; AG Rails Extended for AG Rotation of MCTV.

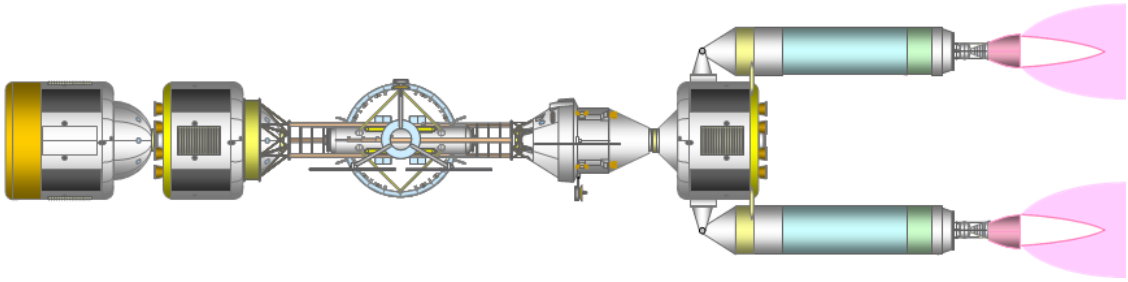

j. Mars Capture – AG Rails Retract to Minimum Position; Mars Orbit Insertion Burn using (2) MTS.

Figure 10. Mission Description, Continued – TMI through Lander Docking to MCTV.

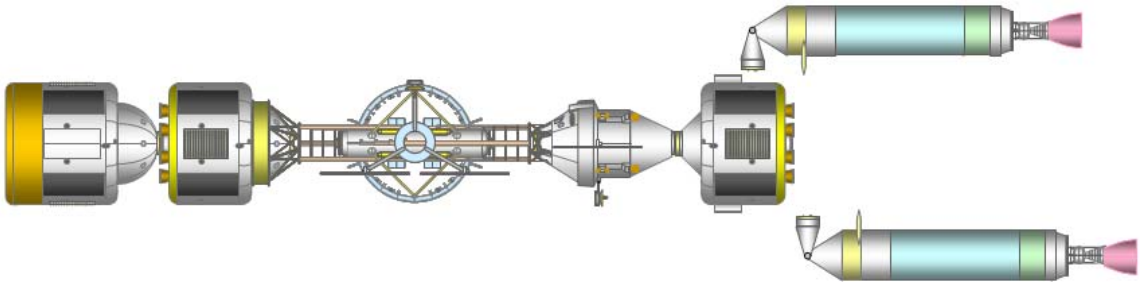

k. Aerobraking – (2) Mars Transfer Stages Jettisoned in Mars Capture Orbit.

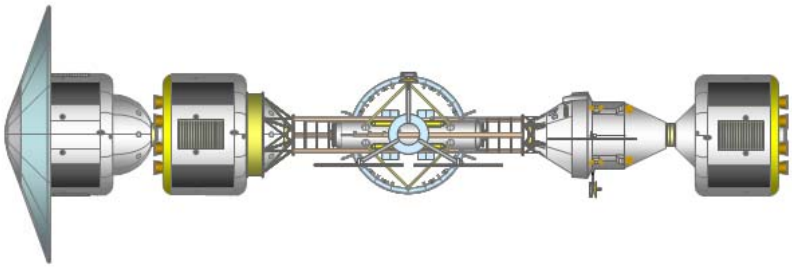

l. Aerobraking – DSV2 Inflatable Heatshield Extension Deployed in Preparation for Aerobraking.

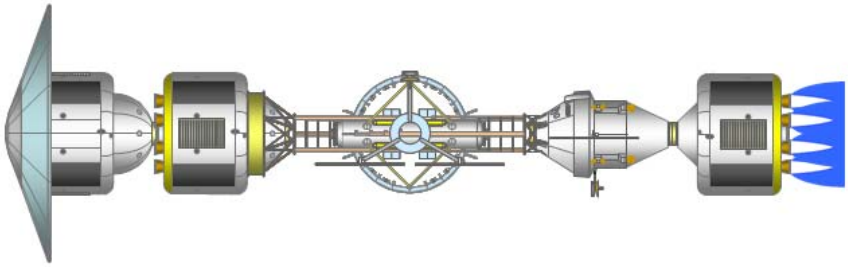

m. Aerobraking – Aerobraking "Walk-In" Burn, to Lower Orbit Periapsis, Performed by DSV3.

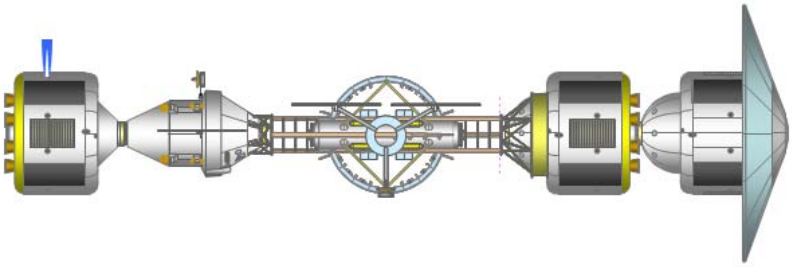

n. Aerobraking – Aerobraking "Trim" Burn, to Adjust Orbit Periapsis and Density, Performed by DSV3.

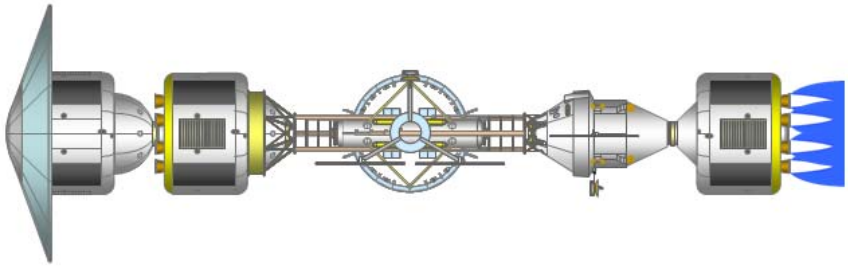

o. Aerobraking – Circularization Burn, to Raise Orbit Periapsis and End Aerobraking, Performed by DSV3.

Figure 10. Mission Description, Continued – TMI through Lander Docking to MCTV.

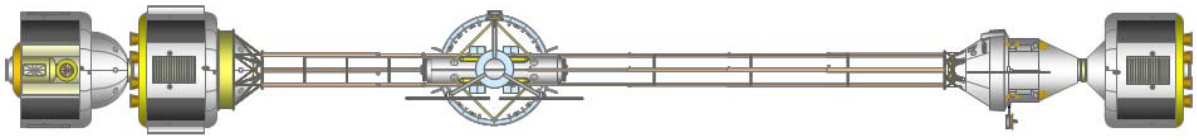

p. Mars Parking Orbit – AG of MCTV in 500 km Mars Parking Orbit Waiting for Arrival of (2) MLTVs.

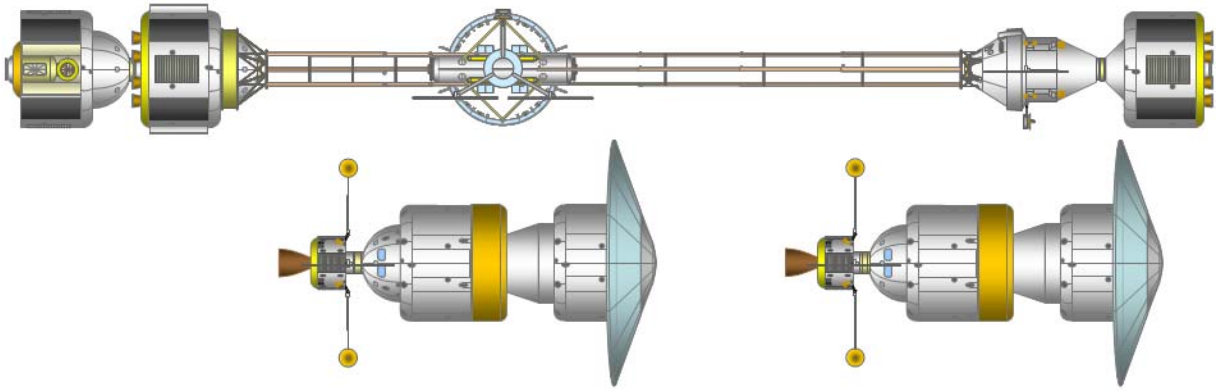

q. Mars Parking Orbit – MCTV Stops AG Rotation; (2) MLTVs Rendezvous with MCTV.

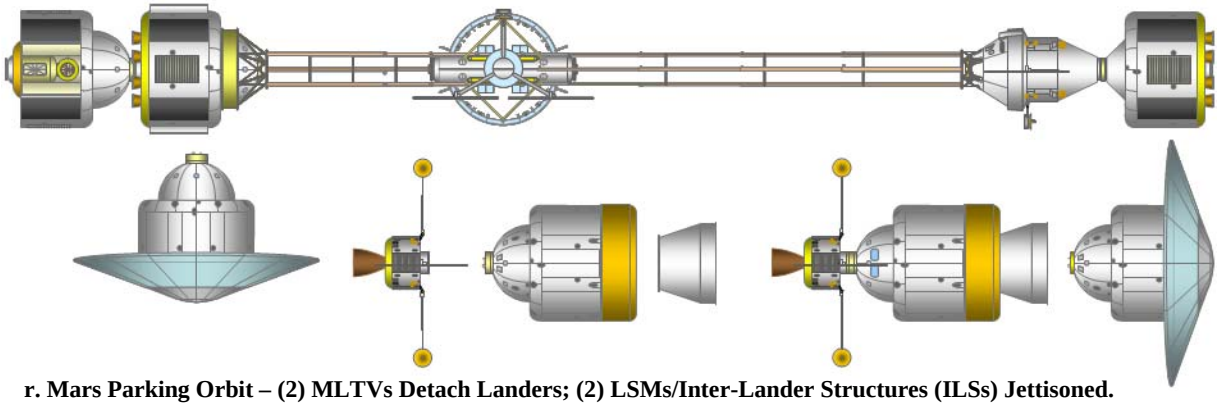

r. Mars Parking Orbit – (2) MLTVs Detach Landers; (2) LSMs/Inter-Lander Structures (ILSs) Jettisoned.

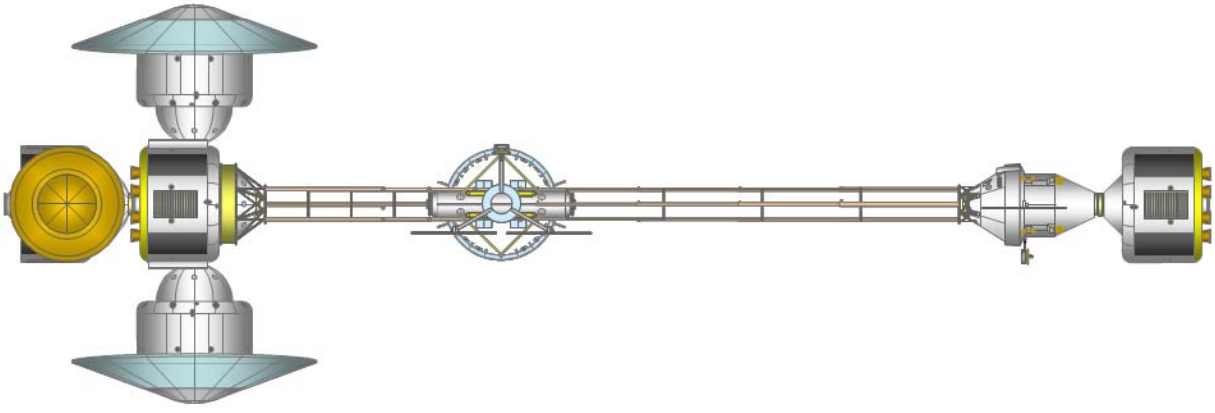

s. Mars Parking Orbit – (4) Mars Landers Docked to MCTV; Preparing for Mars Surface Exploration Mission.

Figure 10. Mission Description, Continued – TMI through Lander Docking to MCTV.

Table 8. MCTV Performance for TMI, MOI, and Aerobraking (A/B) Burns.

MCTV Mass (kg)	TMI Burn A	TMI Burn B	TMI Burn C	MOI Burn	A/B Burns
Items Launched by SLS3					
AGM	5,475	5,475	5,475	5,475	5,475
(4) Crew w/ Suits, ELSS, & PLSS	0	0	0	660	660
DSV1 Inert, Payload, & Propellant	29,766	29,766	29,766	29,766	29,766
DSV1 LSS Consumables	7,234	7,234	7,234	7,234	7,234
DSV1 Total Mass	37,000	37,000	37,000	37,660	37,660
EDS3 Non-Propellant	8,600	Jettisoned			
EDS3 Usable Propellant [2]	77,400				
EDS3 Total Mass	86,000				
Total Mass	128,475	42,475	42,475	43,135	43,135
Items Launched by D4H3					
MTS-C1, MRA1 [1], MAS1 Inert	3,300	3,300	3,300	3,300	Jettisoned
MTS-C1 Usable Propellant [2, 3]	24,300	24,300	24,300	10,645	
Total Mass	27,600	27,600	27,600	13,945	
Items Launched by SLS4					
DSV3 Inert & Payload	2,635	2,635	2,635	2,635	2,635
DSV3 Usable Main/RCS Prop. [2]	14,140	14,140	14,140	13,560	13,560
DSV3 Total Mass	16,775	16,775	16,775	16,194	16,194
DSV2 to DSV3 Adaptor (ILS)	1,000	1,000	1,000	Jettisoned	
DSV2 Inert & Payload	5,209	5,209	5,209	5,209	5,209
DSV2 LSS Cons. & Us. RCS Prop.[2]	15,365	15,365	15,365	11,773	11,773
DSV2 Total Mass	20,575	20,575	20,575	16,983	16,983
EDS4 Non-Propellant	8,600	8,600	Jettisoned		
EDS4 Usable Propellant [2]	77,400	77,400			
EDS4 Total Mass	86,000	86,000			
Total Mass	124,349	124,349	38,349	33,177	33,177
Items Launched by D4H4					
MTS-C2, MRA2 [1], MAS2 Inert	3,300	3,300	3,300	3,300	Jettisoned
MTS-C2 Usable Propellant [2, 3]	24,300	24,300	24,300	10,645	
Total Mass	27,600	27,600	27,600	13,945	
Items Launched by D4H5					
(4) Crew w/ Suits, ELSS, & PLSS	660	660	660	0	0
MPCV and MDA Non-Payload	21,382	21,382	21,382	21,382	21,382
MPCV Docking Adaptor (MDA)	1,000	1,000	1,000	1,000	1,000
Total Mass	23,042	23,042	23,042	22,382	22,382
Total Vehicle					
MCTV Stack Initial Mass	331,066	245,066	159,066	126,583	98,694
MCTV Stack Final Mass	253,666	167,666	132,873	105,294	94,795
Propellant Mass Consumed	77,400	77,400	26,193	21,289	3,899
Velocity Change (m/s)					
Burn Net δV	1,217	1,735	822		
Total δV TMI [4]			3,774		
Total δV MOI [4, 5]				842	
Total δV Aerobraking Phase [4]					129
Acceleration (m/s^2 or g's)					
Initial Acceleration (m/s^2)	1.997	2.698	2.771	3.483	1.099
Initial Acceleration (g_{0Earth})	0.203	0.275	0.282	0.355	0.112
Final Acceleration (m/s^2)	2.607	3.944	3.318	4.187	1.145
Final Acceleration (g_{0Earth})	0.266	0.402	0.338	0.426	0.117

[1] 400 kg propellant used (or dumped) per MRA for MTS-C rendezvous and docking with MCTV prior to TMI.
[2] Usable propellant masses exclude residuals. [3] 1,118 kg of propellant lost to boil-off prior to MOI by (2) MTS-C.
[4] Includes 2% Flight Performance Reserve. [5] Includes 25 m/s for OTO course correction burns.

C. MCTV Mars Orbit Operations and Landing Mission Description and Performance

1. MCTV Operations in Mars Orbit

The TEI launch window opens ~16 months after MOI. Two months have been allocated to aerobraking and lander rendezvous. The crew will nominally spend the next 11 months exploring the surface of Mars, and spend the last three months in the MCTV in parking orbit waiting for TEI. In the event of an aborted landing, the MCTV has sufficient LSS consumables to support the crew in orbit for the full 16 month duration. After lander departure and return of the crew, the MCTV will be rotated for AG operations using the same procedure described in section IV.B for the outbound transit, at a nominal 3.438 RPM to provide 0.378 Earth g's (Mars surface equivalent) at the DSV2 mid-level crew quarters. A total of two spin-up/spin-down cycles have been allocated for the Mars Parking Orbit phase, and sufficient RCS propellant mass (329 kg) has been reserved in DSV2 and the DSV3 for this purpose.

2. Mars Entry, Descent, and Landing

The Mars Entry, Descent, and Landing (EDL) sequence for the Mars Personnel Lander (MPL) and Mars Cargo Landers (MCLs) is described in detail in Ref. 6. Figures 11a-b and 12a-f show the EDL sequence of events. Four landers, three MCLs and one MPL, are sequentially sent to the surface. The MCLs, two with a habitat (MCL-H), and the other carrying a large pressurized rover (MCL-R), are first prepared for flight operations. The two MCL-Hs, with their inflatable heatshield extensions (HSEs) already deployed from the aerobraking phase, undock from the MCTV and proceed to the surface as shown in Fig 12a. The MCL-R, with its HSE still stowed, undocks later. The inflation sequence of the HSE is shown in Fig. 12b. Each MCL autonomously flies or is remotely piloted to a pre-selected landing zone. The lander maneuvers into the correct attitude for deorbit burn and atmospheric entry. The MPL/MCL landers are designed to land at a MOLA altitude of zero or less from an orbit inclined up to 12.5 degrees from the equator. This will permit a significant amount of Mars' surface to be accessible for exploration. A deorbit burn is accomplished using eight deorbit thrusters as shown in Fig. 12b. This maneuver inserts the lander into an elliptical transfer orbit that dips into Mars' atmosphere at its periapsis of 125 km. Aerodynamic deceleration using the ablative heat shield, also shown in Fig. 12b, begins at an entry interface altitude of 150 km, just before periapsis. This phase continues until the lander has been slowed to Mach (M) = 3.0 at an altitude of 13.9 km. At this point the 27 m diameter DGB parachute is deployed by mortar as shown in Fig. 12c. It is fully inflated at M = 2.7 at an altitude of 13.3 km. It slows the lander to a subsonic speed of Mach = 0.76 at 5.5 km altitude. The rigid heat shield, inflatable HSE, and four landing leg doors are then jettisoned and driven away from the lander by eight solid rocket separation motors as shown in Fig. 12d. The landing legs extend and lock for touchdown after the landing leg doors are jettisoned. The DGB parachute is jettisoned at M = 0.74 at 4.4 km altitude and the powered descent (PD) begins. PD features a powered gravity turn phase and a vertical descent phase, both at a constant thrust/weight (T/W) of 2.0, as shown in Fig. 12e. EDL simulations showed that vehicle T/W needed to be at least 1.95 to sufficiently decelerate the vehicle. PD continues with a timed hover phase at T/W = 1.0 at approximately 25 m above the surface, and a soft landing phase (Fig. 12f). There is sufficient propellant carried to hover for a maximum of 10 s to locate and avoid obstacles. After confirmation of successful MCL landings, the crew would enter the MPL and repeat the same set of events, homing on the MCL location and maneuvering during descent to land nearby. The MPL is capable of abort-to-orbit throughout the PD phase, after the lander decelerates below Mach = 0.74 and the heatshield and parachute have been jettisoned. MPL/MCL EDL flight performance data and trajectory simulation results are shown in Ref 6.

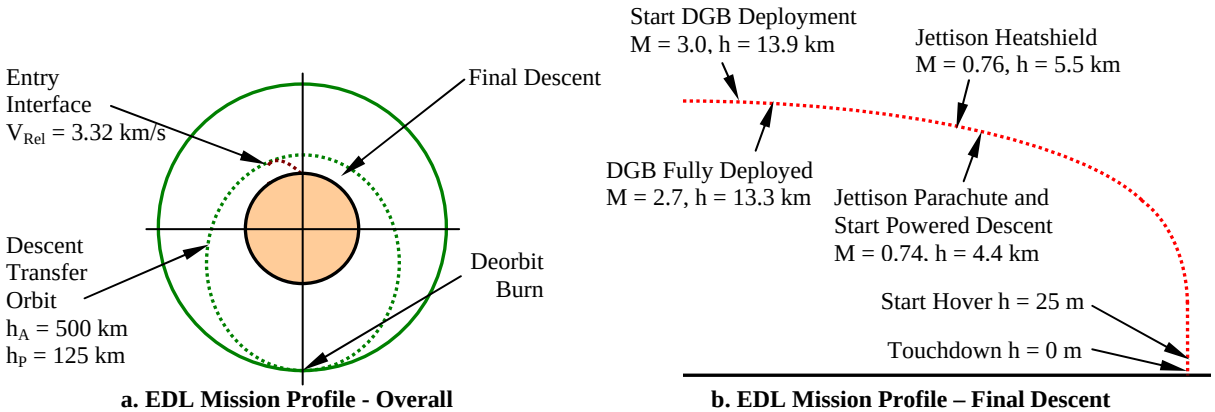

a. EDL Mission Profile - Overall **b. EDL Mission Profile – Final Descent**

Figure 11. MPL/MCL EDL Mission Profile from the 500 km Altitude Parking Orbit to the Surface.

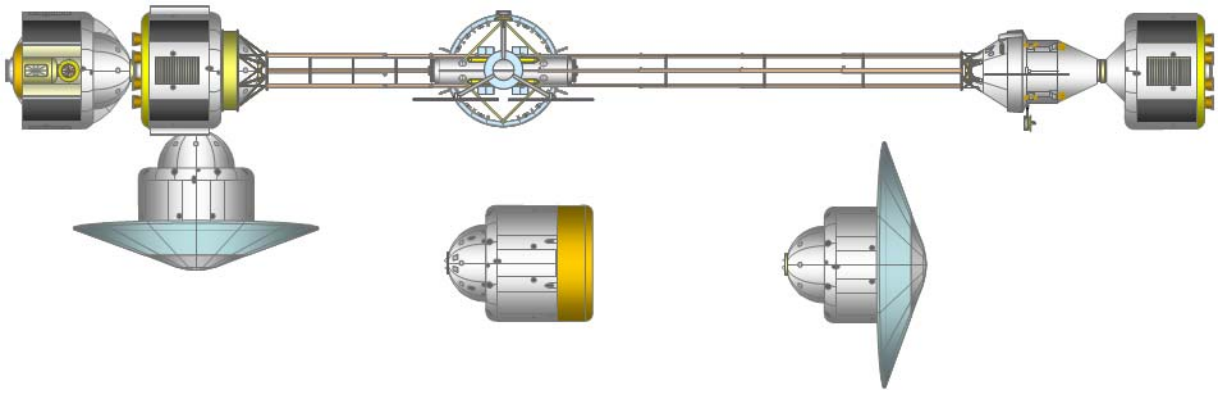

a. Mars EDL – Landers Undock from MCTV; Unmanned Cargo Landers Land before Crew Lands in MPL.

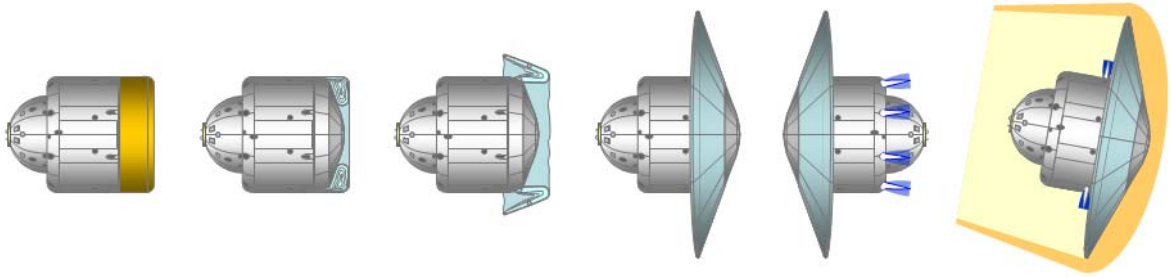

b. Mars EDL – Inflatable Heatshield Extension (HSE), Deorbit Burn, and Atmospheric Deceleration.

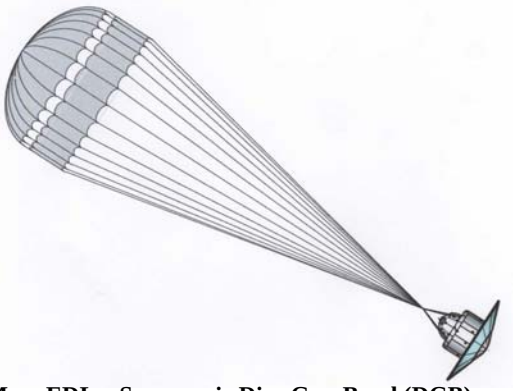

c. Mars EDL – Supersonic Disc-Gap-Band (DGB) Parachute Opens at M = 3.0 (Fully Open at M = 2.7).

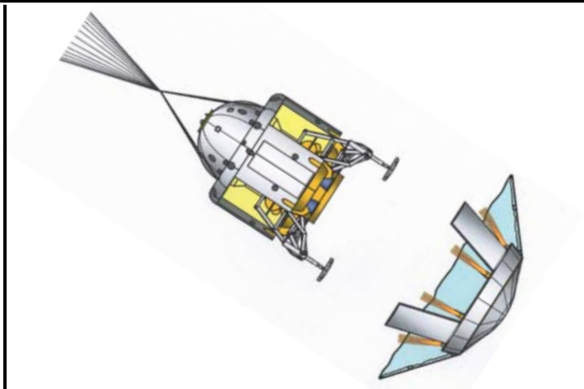

d. Mars EDL – Heatshield, and Landing Gear Doors Jettisoned at M = 0.76; Landing Legs Deployed.

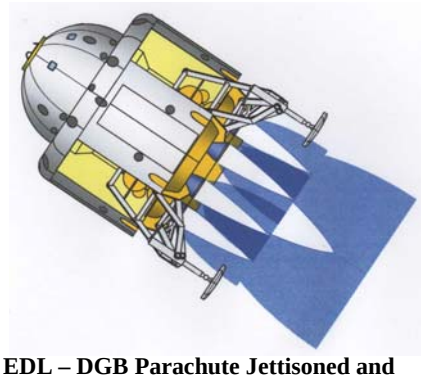

e. Mars EDL – DGB Parachute Jettisoned and Engines Started for Powered Descent at M = 0.74.

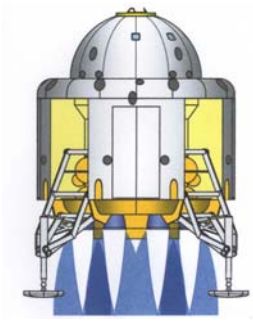

f. Mars EDL – Central Engine Shutdown and Hover (up to 10 s) at h = 25 m; Soft Landing Performed.

Figure 12. Mission Description – Mars Lander Entry, Descent, and Landing (EDL).

3. Mars Surface Operations

The MPL is designed to mate on the surface with multiple MCL-H landers to form a base camp. When mated to the MPL, the two MCL-H landers provide additional LSS consumables for an 11 month surface duration for four crew members. The three MCLs land first and traverse to a rendezvous point, awaiting the MPL arrival. Ideally the MPL should land as close as possible to the MCL site to minimize the distance the MPLs need to traverse, but not close enough to where the exhausts from the MPL descent engines could damage the MCLs during PD. A minimum separation of 200 meters should be adequate. Although the MCL is able to traverse up to 1.0 km per day, the MPL must land within 24 km of the MCL to achieve a linkup before its consumables run low. Dust storms or bad terrain could limit the distance that the MCLs could traverse in 24 days. As a reasonable upper limit, the separation distance should not exceed 10 km. Accurate navigation during the descent and landing is, therefore, required to achieve the 11 month extended mission duration. Precision landing systems for Mars landers, including aerodynamic steering, active terrain sensing, and hi-fidelity powered descent steering and guidance systems are currently being developed for the Mars Science Laboratory and future unmanned Mars landers to permit a landing accuracy within 10 km of a surface target. Figure 13a shows the MPL and MCL in their landed configurations. Figure 13b shows the MPL mated to two MCL-Hs, using the MCL-H surface docking system (SDS) to connect the vehicles. The SDS includes a tunnel with three degrees-of-freedom to compensate for reasonable variations in pitch, yaw, and elevation. Once mated to the habitat, the crew will have a much larger living space than the cramped MPL crew cabin. They can live in the MCL-H habitable volume of 48.5m^3. This provides 24.3m^3 per person for a four-person crew living in two MCL-Hs. The MCL-R will transport a large pressurized rover as shown in Fig. 13c. This will be detailed in future work. Prior to the crew departing the surface in the MPL ascent section, the MCL-Hs are undocked and driven a safe distance away from the MPL to prevent engine exhaust from blasting off MCL parts which could damage the MPL.

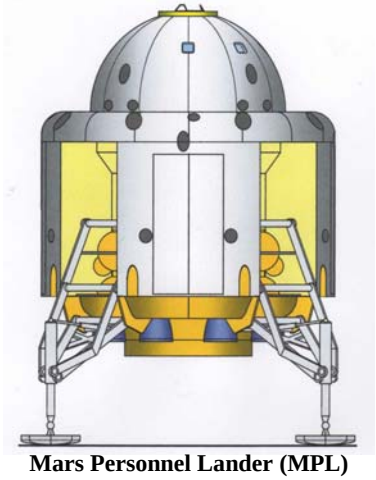

Mars Personnel Lander (MPL)

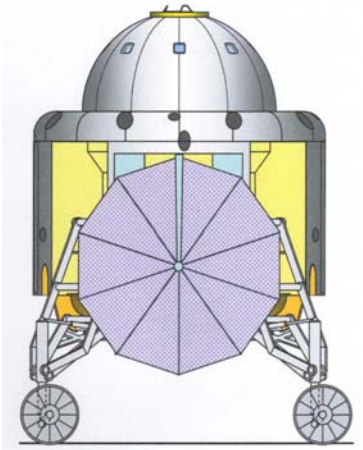

Mars Cargo Lander-Habitat (MCL-H)

a. Mars Surface Operations – Landed Configurations of Mars Personnel and Cargo Landers.

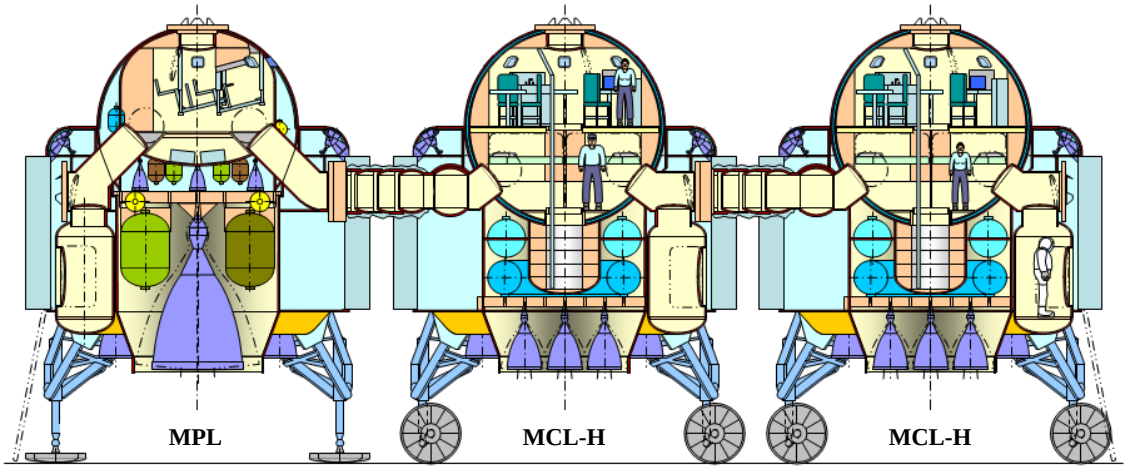

b. Mars Surface Operations –Cutaway Elevation View of MPL Docked to (2) MCL-H (MCL-R Not Shown).

Figure 13. Mission Description – Mars Surface Operations

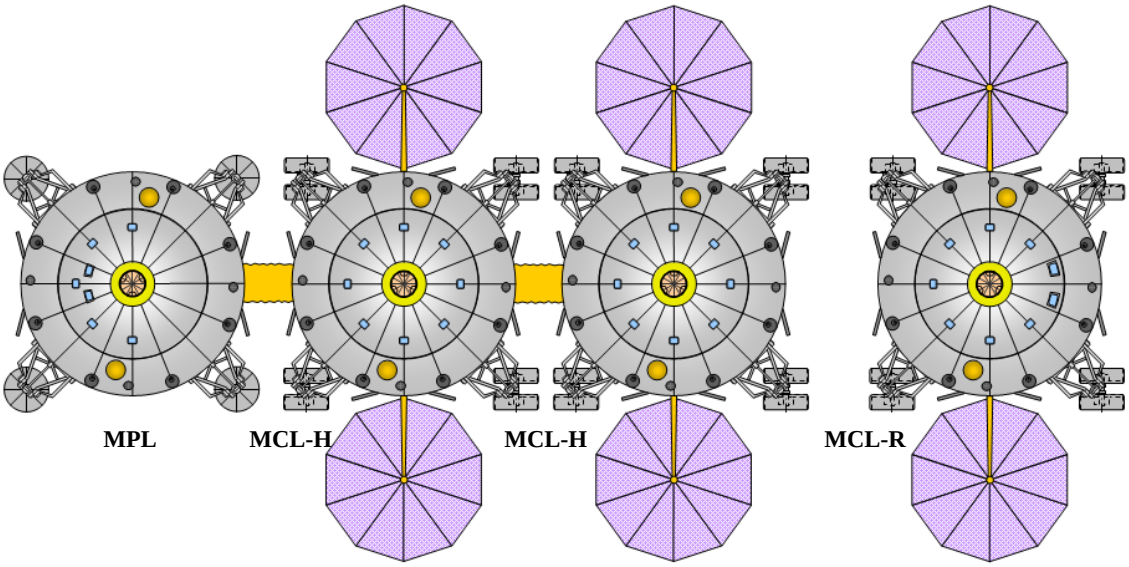

c. Mars Surface Operations – Top View of MPL Docked to (2) MCL-H (MCL-R Shown to the Right).

Figure 13. Mission Description, Continued. – Mars Surface Operations

4. Return of Crew from Surface to Parking Orbit

Figures 14a-b and 15a-g describe the MPL return flight. The MPL ascent trajectory returns the crew from the surface to a 250 km intermediate orbit from launch latitudes between 0.0 and $\pm$12.5 degrees as shown in Fig. 14a. During a normal ascent (or abort to orbit during powered descent), the MPL ascent section (AS) is launched from the Descent Section (DS). Explosive bolts separate the AS from the DS and the AS rises rapidly at a T/W of 2.0 as shown in Figs. 15a and b. The Ascent Booster burn includes an allocation of 120 m/s for a 2.0 degree plane change during ascent to the 250 km orbit. The Ascent Booster, with a simple, reliable, single pressure-fed engine, places the MPL ascent section into the low but stable intermediate circular orbit of 250 km altitude, where the crew has a reasonable chance of being rescued by the MCTV in the event of a failure of the Ascent Orbiter propulsion system. After achieving orbit, the Ascent Booster is jettisoned as shown in Fig. 15c. The Ascent Booster will later reenter due to gradual atmospheric drag and crash onto the surface. The Ascent Orbiter will coast to set up proper initial parameters for the orbit raising maneuver to rendezvous with the MCTV in the 500 km altitude parking orbit. Ascent Orbiter δV includes an allocation of 120 m/s for a 2.0 degree plane change during orbit raising plus 32 m/s for rendezvous and docking for a total of 182 m/s. The crew uses the Orbiter's propulsion system to raise its orbit to the 500 km circular parking orbit using a Hohmann transfer maneuver as shown in Figs. 14b and 15d. The crew then uses the Orbiter's RCS thrusters to rendezvous and dock with the MCTV as shown in Fig. 14e and f. The crew transfers to the MCTV and the Orbiter is jettisoned into the parking orbit as shown in Fig. 14g. Residual propellants will be used to command the spent Ascent Orbiter to modify its orbit in order to provide adequate separation from the MCTV. Eventually, atmospheric drag will also cause its orbit to decay and it will crash onto the surface of Mars.

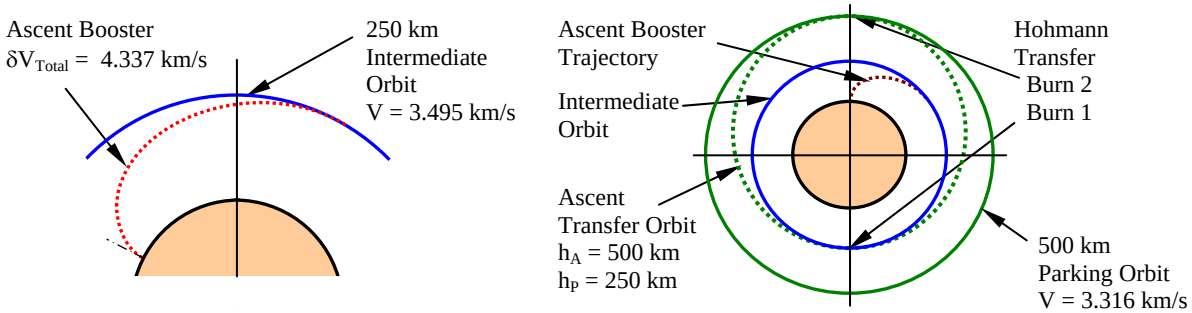

a. Ascent from Surface to Intermediate Orbit **b. Orbit Raising from Intermediate Orbit to Parking Orbit**

Figure 14. MPL Ascent Mission Profile from Mars Surface to the 500 km Parking Orbit.

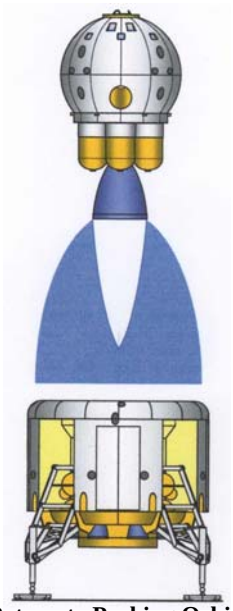

a. Return to Parking Orbit – MPL Two-Stage Ascent Section (AS) Launches from Descent Section.

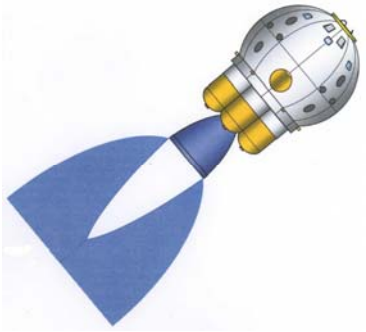

b. Return to Parking Orbit – MPL AS Ascends to 250 km Intermediate Orbit using Ascent Booster Propellant.

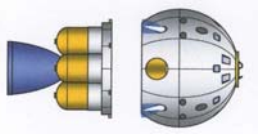

c. Return to Parking Orbit – MPL Spent Ascent Booster Jettisoned in Intermediate Orbit.

d. Return to Parking Orbit – MPL Ascent Orbiter Ascends to Parking Orbit using Hohmann Transfer.

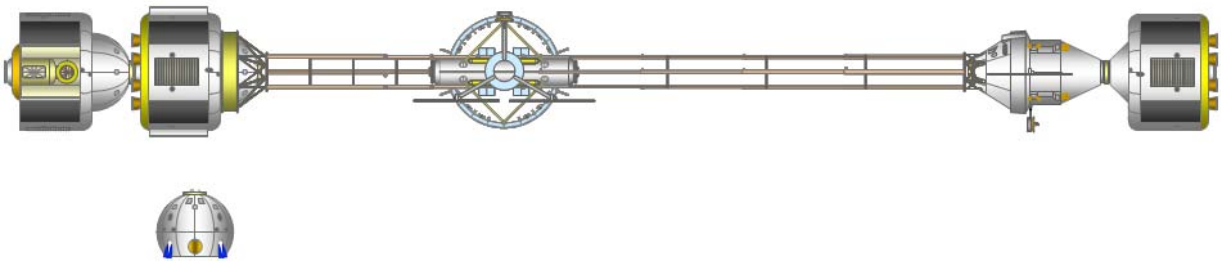

e. Return to Parking Orbit – MPL Ascent Orbiter Rendezvous with MCTV.

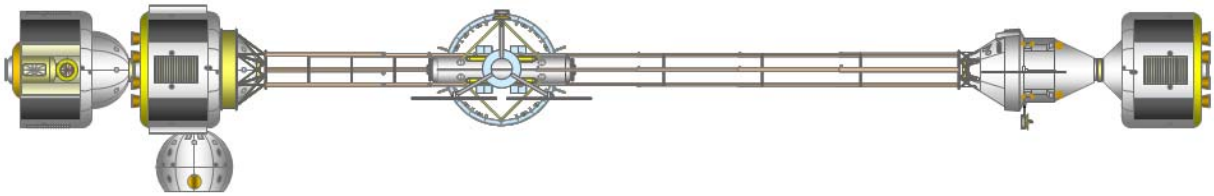

f. Return to Parking Orbit – MPL Ascent Orbiter Docks with MCTV; Crew Transfers to MCTV.

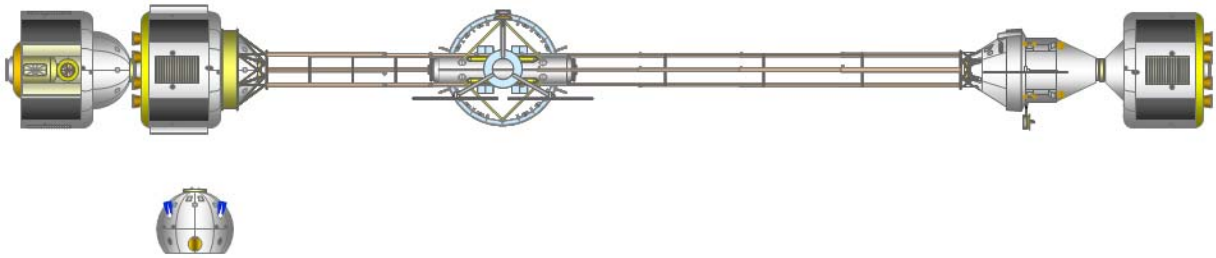

g. Return to Parking Orbit – MPL Ascent Orbiter Jettisoned in Parking Orbit; Landing Mission Concluded.

Figure 15. Mission Description – Crew Ascent from the Surface to the MCTV in Parking Orbit.

D. MCTV Mission Description and Flight Performance, Return to Earth from Mars Parking Orbit

Figures 16 and 17a-q describe the return of the MCTV to Earth from the Mars parking orbit. Figures 17a-c describe preparations for TEI: DSV2 relocates from DSV1 to DSV3. The DSV2 Propulsion Section (PS), containing excess consumables and solid waste, is jettisoned. TEI is performed using three sequential burns to provide sufficient δV. TEI burn A uses the DSV1 PS propulsion system. This burn puts the MCTV in a highly elliptical escape orbit as shown in Fig. 16 and 17d-e. The DSV2 Habitat Section then relocates to DSV1, as shown in Figs. 17 f-g, during the 15.64 hr period escape orbit. TEI burn B is performed by DSV3 at the periapsis of the escape orbit, and TEI burn C is performed by the MPCV immediately following TMI Burn B, as shown in Figs. 16 and 17h-j. The four-person crew will continue to have 24.3m^3 of habitable volume per person, using the combined habitation volume of DSV1 and DSV2. The Mini-Mag radiation shield is continuously energized throughout the ~210 day inbound transit. The MCTV will be spun up for AG operations as shown if Fig. 17k, using the same procedure described in section IV.B for the outbound transit, at a nominal 3.333 RPM to provide 0.378 Earth g's (Mars surface equivalent) at the DSV2 mid-level crew quarters. The MCTV will be spun-down for inbound course correction (ICC) burns and re-spun up after the conclusion of the ICC burns. A total of four spin-up/spin-down cycles have been allocated for the inbound transit, and sufficient RCS propellant mass (256 kg) has been reserved in DSV2 and the MPCV for this purpose. The MPCV will perform all ICC burns during the inbound transit.

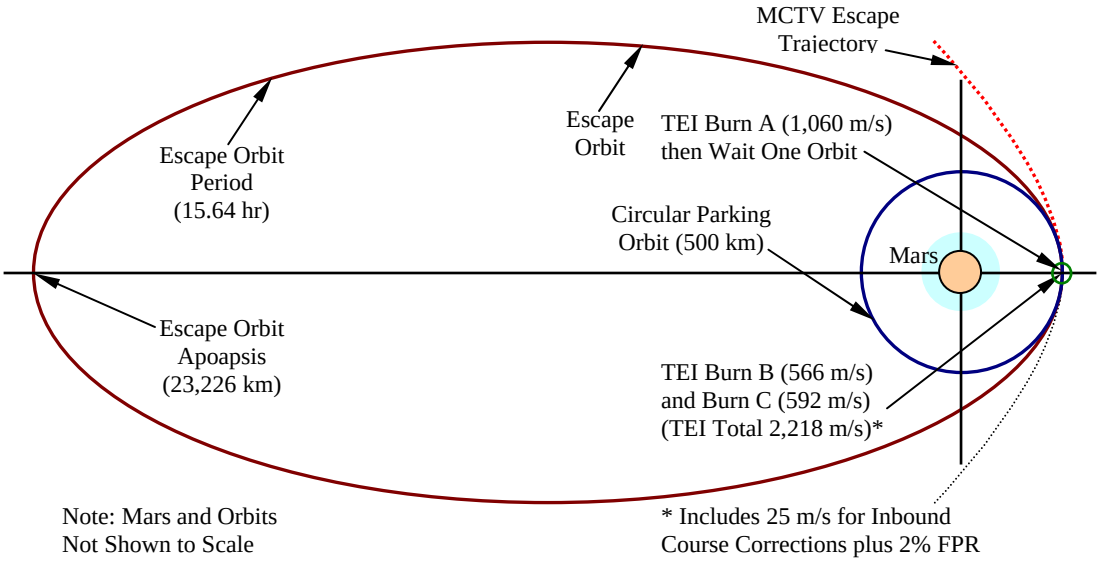

Figure 16. MCTV TEI Burn A, Escape Orbit, and TEI Burns B and C into Mars Escape Trajectory

Figure 17l shows the MCTV approaching Earth. The vehicle has passed within the Earth's 924,133 km activity sphere radius, where the gravitational influence of the Earth exceeds the gravitational influence of the Sun. The crew is now less than two days from Earth. The MCTV is spun-down to 0 RPM and the Mini-Mag coil is de-energized. The DSV1 and MPCV AG rails fully retract and the DSV1 and MPCV dock to the AGM. The crew departs DSV1/DSV2, transports Mars samples into the MPCV, and prepares the MPCV for the return to Earth. Latches on the MPCV AG rail-to-vehicle interface unlock and disengage from the six Launch Abort System hardpoints on the MPCV. The MPCV undocks and separates from the AGM/DSV1/DSV2 stack as shown in Fig. 17m. This occurs at a radius of approximately 800,000 km, when the MPCV is approximately 36 hours away from the entry interface point at an Earth periapsis altitude of 125 km. The MPCV adjusts its trajectory towards Earth by performing Entry Corridor Control (ECC) burns with its primary axial thrusters, and main engine if needed, as shown in Fig. 17n. The MPCV Service Module (SM) is jettisoned just before the MPCV reaches the entry interface point as shown in Fig. 17o, and the SM will burn up in the atmosphere. The MPCV performs a hyperbolic direct entry as shown in Fig. 17p, using the Earth's atmosphere to decelerate. The MPCV is recovered using parachutes in an ocean landing as shown in Fig 17q, and the crew and MPCV are picked up by recovery vessels. The bulk of the AGM/DSV1/DSV2 stack will also burn up in the atmosphere, with its entry targeted at an area of open ocean to avoid debris landing in populated areas. This is the conclusion of the Mars exploration mission, however it remains to be determined if the crew and Mars samples will need to be quarantined as was done for the Apollo 11, 12, and 14 Moon landing missions. Table 9 provides a summary of MCTV flight performance data for the TEI and ECC burns.

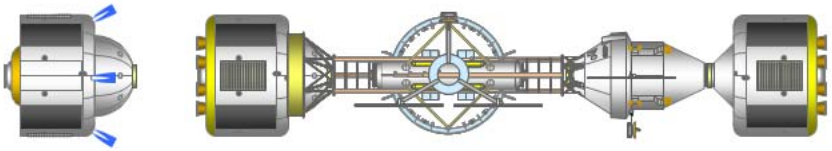

a. Mars Departure – AG Rails Retract to Minimum Position; DSV2 Undocks From DSV1.

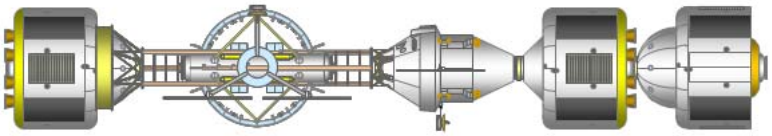

b. Mars Departure – DSV2 Docks to DSV3 Aft Docking Fixture.

c. Mars Departure – DSV2 Propulsion/Consumables Section Jettisoned (Includes Excess Food and Waste).

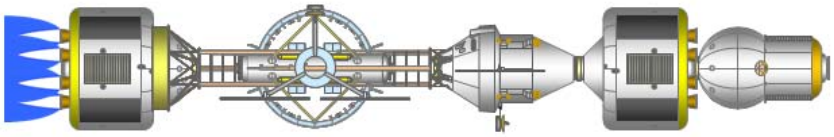

d. Mars Departure – DSV1 Performs Trans-Earth Injection (TEI) Burn A.

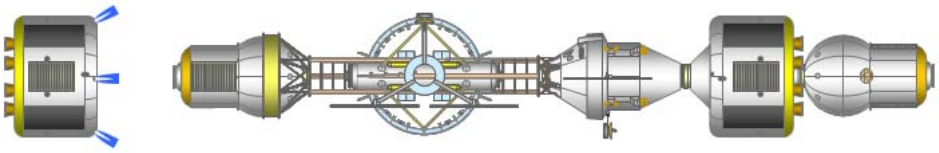

e. Mars Departure – Spent DSV1 Propulsion Section Jettisoned; MCTV now in Elliptical Escape Orbit.

Figure 17. Mission Description – MCTV Return from Mars Parking Orbit to Earth.

f. Mars Departure – MCTV in Escape Orbit; DSV2 Habitat Section Undocks from DSV3.

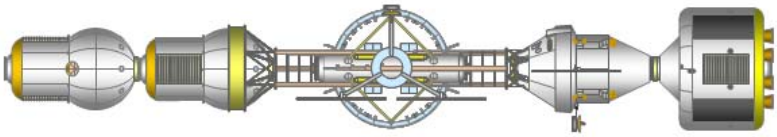

g. Mars Departure – MCTV in Escape Orbit; DSV2 Habitat Section Re-docks to DSV1 Aft Docking Hatch.

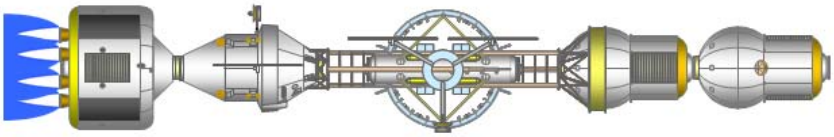

h. Mars Departure – MCTV in Escape Orbit; Vehicle Rotated 180 Degrees; TEI Burn B using DSV3.

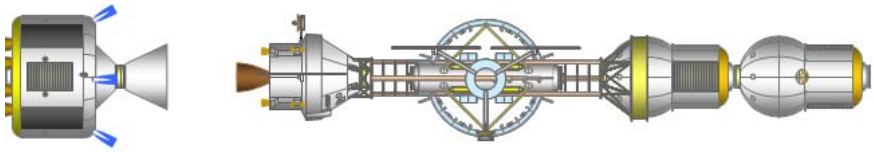

i. Mars Departure – MCTV in Escape Orbit; Spent DSV3 and MPCV Docking Adaptor (MDA) Jettisoned.

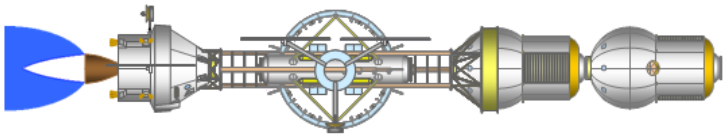

j. Mars Departure – MCTV in Escape Orbit; TMI Burn C using MPCV Propulsion System.

Figure 17. Mission Description, Continued – MCTV Return from Mars Parking Orbit to Earth.

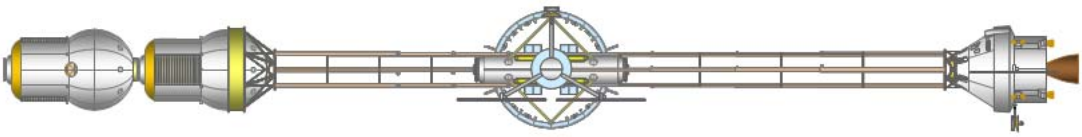

k. Inbound Transit – AG Rails Extend for AG Rotation of MCTV.

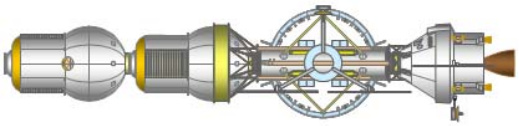

l. Earth Return : Spin-Down to 0 RPM; Mini-Mag Deenergized; AG Rails Retract; Crew Xfer. to MPCV.

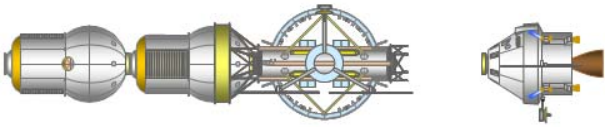

m. Earth Return: DSV2, DSV1, & AGM Jettisoned.

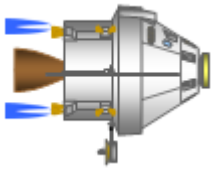

n. Earth Return: MPCV Entry Corridor Control Burn.

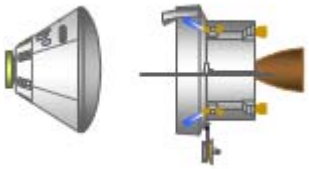

o. Earth Return: MPCV Service Module Jettisoned.

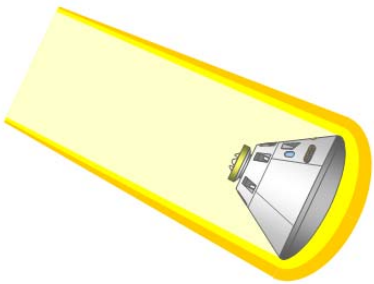

p. Earth Return: MPCV Crew Module Direct Entry.

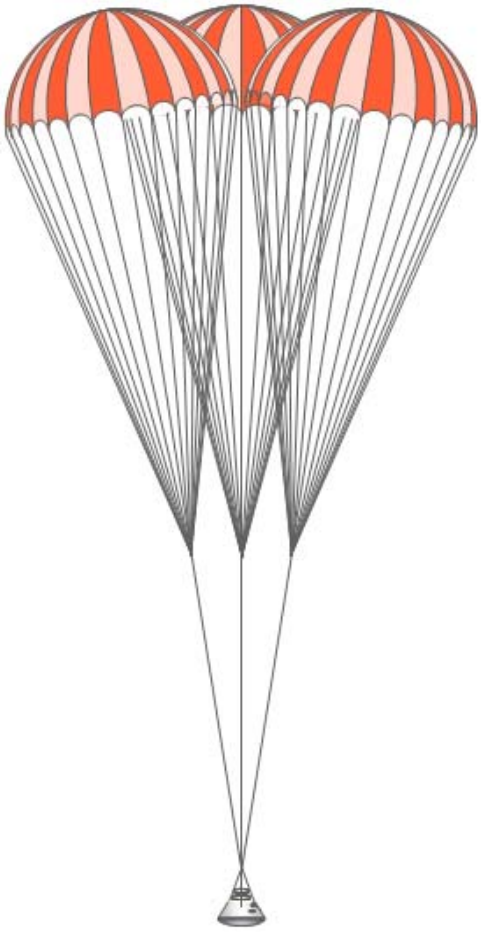

q. Earth Return: Crew Module Parachute Recovery.

Figure 17. Mission Description, Continued – MCTV Return from Mars Parking Orbit to Earth.

Table 9. MCTV Performance for TEI and Entry Corridor Control (ECC) Burns.

MCTV Mass (kg)	TEI Burn A	TEI Burn B	TEI Burn C	ECC Burn
DSV2				
DSV Crew Habitat (HS) Total	6,547	6,547	6,547	
Propulsion Stage (PS) Total	Jettisoned			
DSV2 Total Mass	6,547	6,547	6,547	Jettisoned
DSV1				
HS Payload [1]	500	500	500	
HS Inert Mass	2,520	2,520	2,520	
HS LSS Consumables	7,234	7,234	7,234	
Habitat Stage Subtotal	10,254	10,254	10,254	
PS Payload (Airlock)	400			
PS Inert Mass	2,599			
Usable RCS Propellant Mass [2]	50			
PS Operating Empty Mass	3,049			
Usable Main Propellant Mass [2]	23,738			
Propulsion Stage Subtotal	26,787	Jettisoned		
DSV1 Total Mass	37,041	10,254	10,254	Jettisoned
AGM				
AGM Total Mass	5,475	5,475	5,475	Jettisoned
MPCV				
Payload Mass [1]	0	0	0	500
MPCV Inert Mass	13,475	13,475	13,475	13,475
MPCV Operating Empty Mass	13,475	13,475	13,475	13,975
MPCV Usable Propellant Mass [2]	7,907	7,907	7,907	246
MPCV Total Mass	21,382	21,382	21,382	14,221
MDA				
MPCV Docking Adaptor (MDA)	1,000	1,000	Jettisoned	
DSV3				
Inert Mass	2,135	2,135		
Usable RCS Propellant Mass [2]	50	25		
Operating Empty Mass	2,185	2,160		
Usable Main Propellant Mass [2]	9,245	9,245		
DSV3 Total Mass	11,429	11,404	Jettisoned	
Total Vehicle				
MCTV Stack Initial Mass	82,875	56,063	43,658	14,221
MCTV Stack Final Mass	59,137	46,818	36,125	13,975
Propellant Mass Consumed	23,738	9,245	7,533	246
Velocity Change (m/s)				
Burn Net δV	1,064	571	584	
Total δV TEI [3, 4]			2,219	
Total δV ECC [3, 5]				56
Acceleration (m/s^2 or g's)				
Initial Acceleration (m/s^2)	1.309	1.935	0.765	2.348
Initial Acceleration (g_{0Earth})	0.133	0.197	0.078	0.239
Final Acceleration (m/s^2)	1.835	2.318	0.924	2.390
Final Acceleration (g_{0Earth})	0.187	0.236	0.094	0.243

[1] (4) Crew w/ Spacesuits, and ELSS, and 20 kg of Return Samples; [2] Usable propellant masses exclude residuals.
[3] Includes 2% Flight Performance Reserve. [4] Includes 25 m/s for ITO course correction burns.
[5] ECC Burn includes 25 m/s for main burn and 30 m/s Mission Reserve, plus 2% FPR = 56 m/s.

V. Design of MEV Architecture Components

A. Design of Mars Transfer Stage (MTS)

A Centaur-derived Mars Transfer Stage (MTS) has been designed for the MEV architecture with a near-term solution based on proven technology and existing engines. It is utilized on both the MLTV and MCTV to perform the final TMI burn and MOI burn. Along with reliability, the MTS mass fraction, boil-off and ISP are critical parameters affecting the mission performance,[11] as shown in Fig. 18. Centaur's inherently high thermal and mass efficiency make it the ideal foundation from which to develop the MTS that will enable mankind to venture beyond the Earth-Moon system. Today's Centaur has a propellant mass fraction (f_P) of 0.90 and has demonstrated 2% per day boil-off rate.[12] With 199 flights spanning 5 decades and 99 consecutive successes, including the November 2011 launch of the Mars Science Laboratory, Centaur provides the demonstrated reliability that will be critical to ensuring that astronauts are delivered safely into Mars orbit by successfully executing the critical Mars Orbit Insertion burn.

To enhance Centaur's ability to support the MEV mission requirements, its weight should be further reduced, the thermal protection system must be enhanced, and the propulsion system must be upgraded. Centaur is a monocoque, pressure stabilized stage with a dry mass of 2,200 kg. The tank walls are stainless steel sheet (0.51 mm (0.020 in)) thick. Centaur was structurally designed for launching 21t payloads with high maximum dynamic pressure (43.1 kPa (900 lb/ft^2)). With attention to how the MTS is launched it can be designed around the orbital environment and ease of manufacture rather than the launch environment. With reduced environments Centaur's wall thickness can be reduced to an historic (0.330 mm (0.013 in.)) The thinner wall thickness also reduces the structural thermal mass and wall conductivity enhancing cryogenic fluid management. By integrating the MTS and Mars mission module avionics and power one can avoid duplication, further reducing the MTS mass.[12] Such integration allows removal of Centaur's battery, flight computer and communications antenna.

To enable the long duration mission required for the MTS, Centaur's thermal protection system will have to be substantially enhanced, reducing boil-off by a factor of 100,[13] while not adding substantial weight, as shown in Fig. 19. Centaur's spray on foam insulation will be replaced with a ground helium-purged integrated multi-layer insulation (IMLI) system. This IMLI system is composed of 40 layers of widely spaced MLI, intermixed with 3 gaseous hydrogen vapor-cooled shields. The IMLI system also provides protection from micrometeoroid damage.

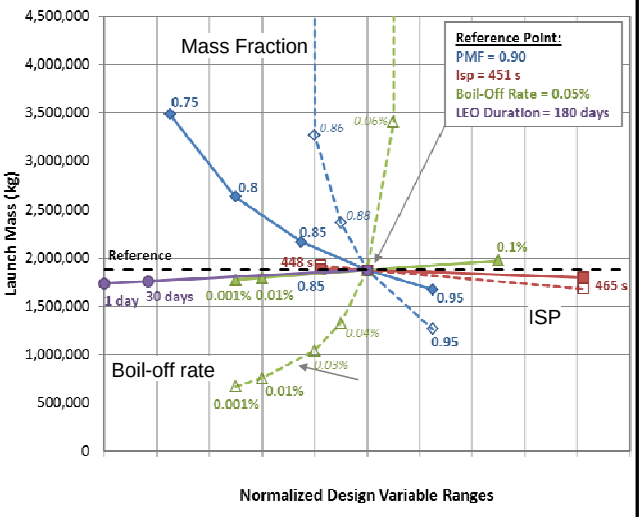

Figure 18. For the MTS, Mass Fraction, Boil-off, and ISP Strongly Affect Mission Performance.

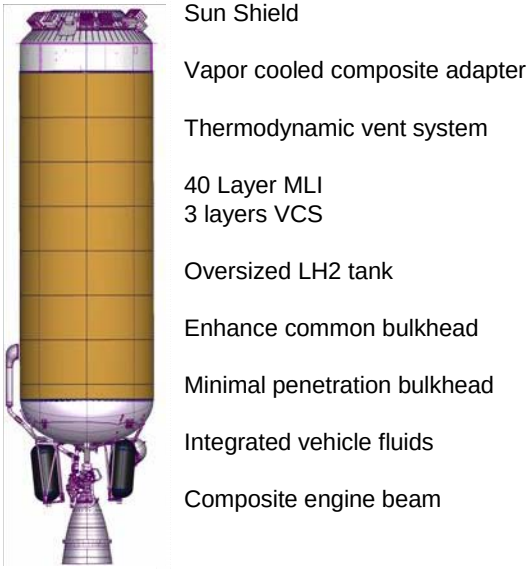

Figure 19. Centaur Thermal Protection System will be Enhanced to Enable Long-Duration Mars

Centaur's common bulkhead will be enhanced with a thicker, improved spacer that ULA demonstrated in 2008. A thermodynamic vent system (TVS) will be included in Centaur's LH_2 tank to enable tank pressure control during settled or zero-G coasts. This TVS will be derived from hardware qualified for the Shuttle Centaur. The slow ~5

Kg/day flow of hydrogen out of the TVS will be used to vapor cool the forward composite adapter, the common bulkhead periphery, LO_2 tank, IMLI vapor-cooled shields and the engine beam. The GH_2 cooling flow around the LO_2 tank will be metered to enable zero LO_2 boil-off without freezing the LO_2.

Centaur's helium pneumatic system and hydrazine reaction control system will be replaced with the in-development integrated vehicle fluid (IVF) system.[14] The IVF will be supported off of Centaur's vapor cooled RL10 engine beam eliminating dozens of aft bulkhead penetrations, enabling zero boiloff LO_2 storage. IVF will compress and store the warm GH_2 from the vapor cooling system to enable attitude control, mid-course corrections and hydrogen tank pressurization. Replacement of Centaur's helium and hydrazine bottles enables replacement of the RL10A-4-2 with the RL10-B-2. The RL10-B-2 will increase the specific impulse (I_{SP}) from RL10A-4-2's 451s to 465.5s. The combination of reduced tank skin gauge, removal of Centaur avionics, enhanced thermal protection, IVF, and replacement of the RL10A-4-2 with the RL10-B-2 or next generation engine is anticipated to reduce the Centaur-derived MTS mass to less than 2,000 Kg. These enhancements will result in a MTS with a boil-off of ~0.02%/day, a f_P of 0.91, and an I_{SP} of 465.5s capable of efficiently supporting the Mars requirements. The Centaur-derived MTS utilizes the Centaur enhancements described above, and incorporates the current geometry for tank end domes, with longer tank barrel sections, to create a "stretched" design. The current RL10-B-2 engine, with an extendable, high expansion ratio nozzle, a vacuum I_{SP} of 465.5 s, and a vacuum thrust of 110.2 kN (24,750 lbf) is utilized. In order to satisfy thrust-to-weight requirements, two RL10-B-2 engines are utilized. Eight gaseous helium spheres for LH_2 and LO_2 tank pressurization are located directly above the LH_2 tank, inside the forward tank skirt. The MTS configuration is shown in Fig. 20, and mass and performance data are shown in Tables 2, 7 and 8.

B. Design of Earth Departure Stage (EDS)

The Earth Departure Stage configuration is shown in Fig. 21. The EDS is needed to perform TMI burns for both the MLTV and MCTV. The EDS must be a highly efficient design in order to satisfy multiple requirements: it must be lightweight, with high I_{SP} engines, in order to maximize flight performance and maximize the mass available to the mission payload, and it must be compact, in order to minimize overall stack height inside the SLS payload shroud and maximize the volume available to the mission payload. This will minimize the number of SLS launches and mission overall cost. To minimize parasitic structural mass, a common bulkhead is utilized between the LH_2 and LO_2 tanks. The common bulkhead is hemispherical to maximize structural efficiency and minimize its mass. Tank skirts are minimized in this design, and all loads are transmitted into the propellant tank skins with short, direct load paths. Lightweight Aluminum-Lithium (Al-Li) alloy is envisioned as the primary structural material for the EDS. The EDS design usable propellant mass fraction is 0.90. To maximize performance, the EDS utilizes the existing high performance RL10-B-2 LH_2-LO_2 engines of the same type used for the MTS described above. In order to satisfy thrust-to-weight requirements, the EDS utilizes six of these engines in a circular arrangement. Engine thrust loads are reacted directly into a ring frame which ties directly into the y-joint at the common bulkhead between the LO_2 and LH_2 tanks. Twelve gaseous helium cylinders for LH_2 and LO_2 tank pressurization are located within the LH2 tank. The EDS will also incorporate the advanced ground helium-purged integrated multi-layer insulation system, described above for the Centaur-derived MTS, in order to minimize propellant boil-off during launch, LEO assembly, and TMI operations. The EDS mass and performance data are shown in Tables 2, 7, and 8.

C. Design of Lander Service Module (LSM)

The Lander Service Module configuration is shown in Fig. 22. The LSM has multiple functions. It provides propulsion, power, communications, and guidance, navigation, and control (GN&C), (1) for the MTS-L post-launch, for rendezvous and docking with the MLTV stack during the assembly phase, (2) for the MLTV stack during the outbound transit to Mars, (3) for the aerobraking (A/B) phase. It also provides primary propulsion during A/B, and (4) for rendezvous of the MLTV stack with the MCTV for landers delivery to the MCTV in LMO. The LSM utilizes storable Mono-Methyl Hydrazine (MMH) and Nitrogen Tetroxide (N_2O_4) propellants for main propulsion and RCS. The LSM main engine is the 33.4 kN (7,500 lbf) Orion Main Engine (OME) used on the MPCV Service Module (SM). The LSM Reaction Control System (RCS) utilizes 32x 111 N (25 lbf) 6-axis RCS thrusters and four 557 N (125 lbf) main axial thrusters of the same type used on the MPCV SM. The LSM mounts a pair of 5.5m diameter 6kW Ultra-Flex solar arrays of the same type used on the MCTV AGM and MPCV SM. The LSM also mounts a pair of deep space Communications Transponder Assemblies (CTAs) on extendable masts. The CTA consists of a radio frequency electronics compartment, antenna feed, high gain antenna reflector, and two-axis gimbal mount of the same type used on the MCTV AGM. The LSM Adaptor structure (LAS) structurally connects the LSM to the MTS and reacts launch loads. The LSM mounts an LDA to enable LSM docking to the Lander/EDS stack. The LDA stays with the lander when the LSM is jettisoned. LSM mass and performance data are shown in Tables 2 and 7.

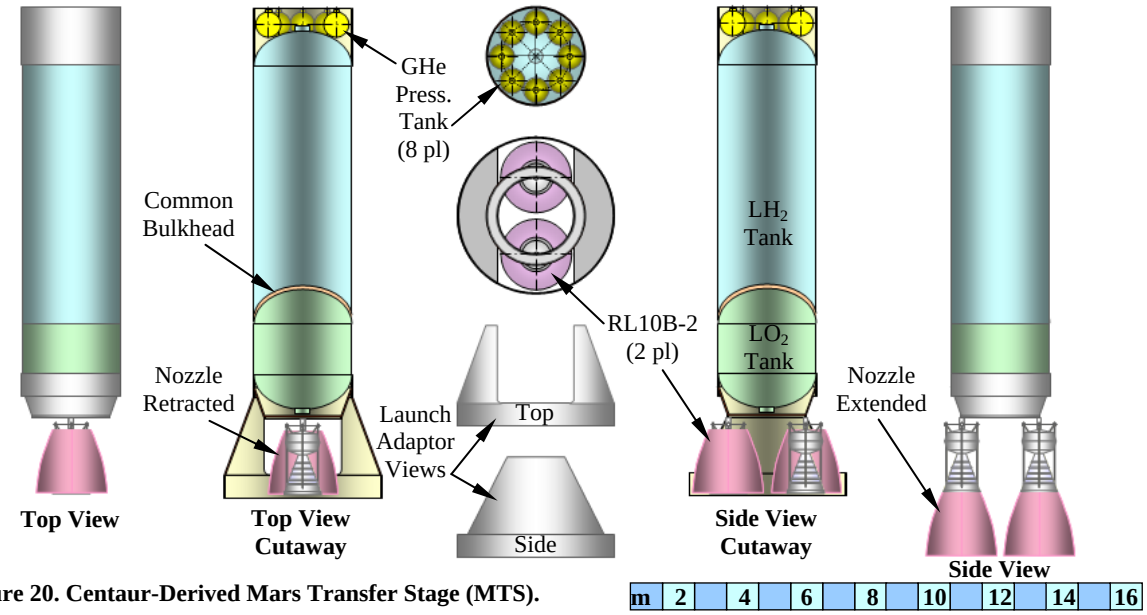

Figure 20. Centaur-Derived Mars Transfer Stage (MTS).

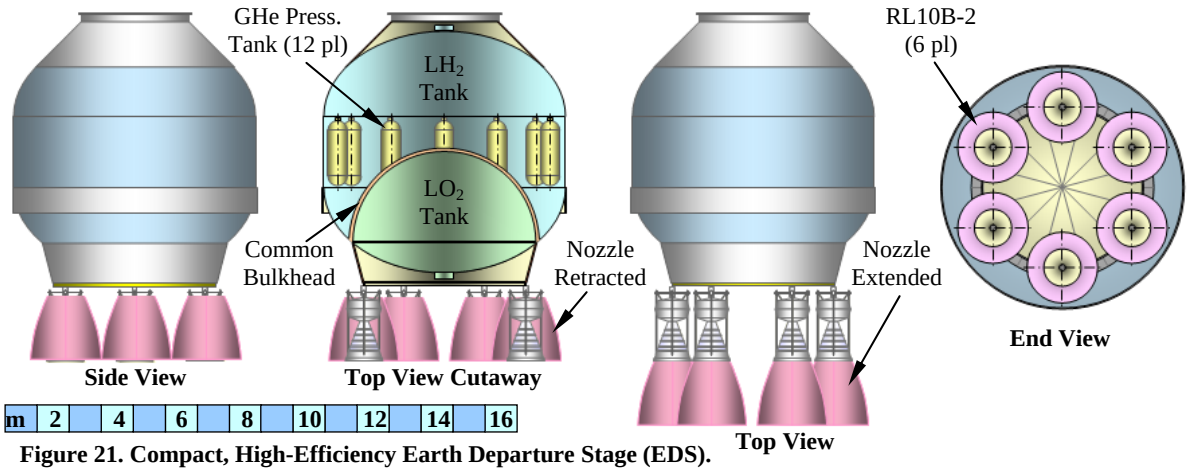

Figure 21. Compact, High-Efficiency Earth Departure Stage (EDS).

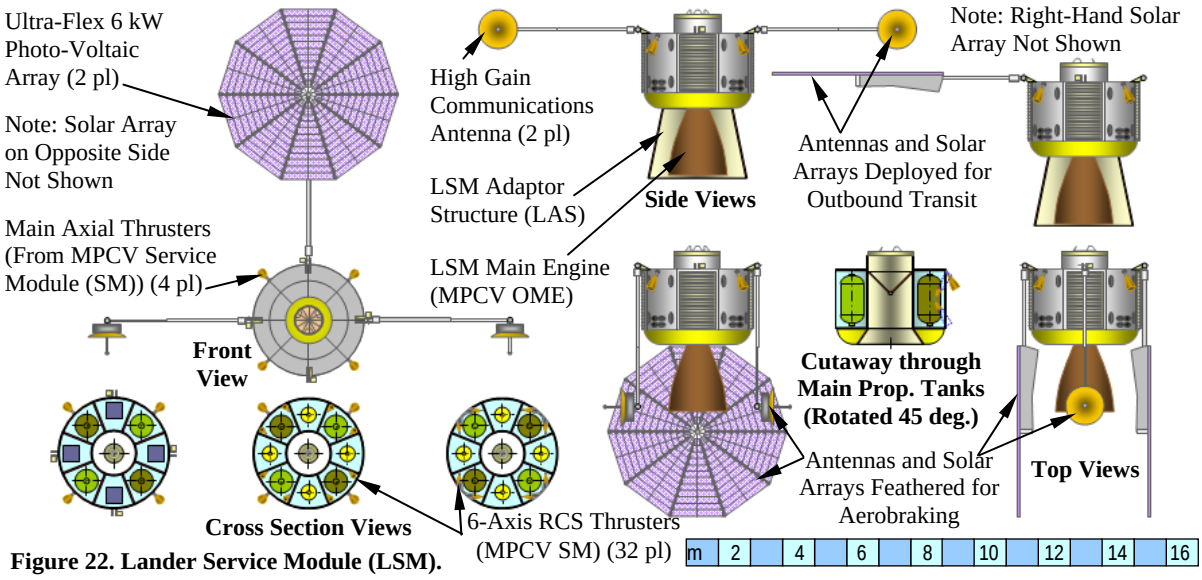

Figure 22. Lander Service Module (LSM).

D. Common Modular Design for Mars Landers and Deep Space Vehicles (DSVs).

Spaceship Discovery is a conceptual space vehicle architecture that utilizes advanced nuclear thermal propulsion to enable human exploration of the solar system.[5] Design reference missions (DRMs) to Earth's Moon, Mars, the asteroid Ceres, and the moons of Jupiter, Ganymede and Callisto, were developed for Spaceship Discovery. A DRM to the largest airless moons of Saturn, Rhea and Iapetus, is under development. Landers were developed to land crew and/or cargo on these bodies: Lander Module 1 (LM1) is a lander designed for the large airless moons Ganymede and Callisto.[15] This lander provides two-way transportation for a two-person crew between orbit and the surface, and life support for a 30 day mission. It can also be flight tested on Earth's moon; Lander Module 2 (LM2) is a piloted crew lander for Mars; The LM2 provides two-way transportation for a three- or four-person crew between Mars orbit and the surface, and provides life support for 81 man-days; Lander Module 3 (LM3) is an autonomous cargo lander for Mars. It provides one-way, autonomous transportation of cargo from Mars orbit to the surface and can be configured to carry a mix of consumables and equipment, or equipment only. The LM3 habitat variant (LM3-HAB) is designed to link up with the LM2 and extend the crew's surface stay for an additional 630 man-days beyond the capability of the LM2. Lander Module 4 (LM4) is a crew exploration lander that is designed to land on the smaller airless bodies Ceres, Rhea, and Iapetus.[16] This lander provides two-way transportation for a two-person crew between orbit and the surface, and life support for 30 days. Figure 23 shows the common modular design utilized for the Spaceship Discovery LM1, LM2, LM3, and LM4 landers. To avoid confusion between the Spaceship Discovery architecture, which uses four landers (LM1, LM2, LM3, and LM4), and the MEV architecture, which uses only the LM2 and LM3, the LM2 crew lander has been renamed the Mars Personnel Lander (MPL), and the LM3 cargo lander has been renamed the Mars Cargo Lander (MCL). The MCTV Deep Space Vehicle (DSV) designs shown in Fig. 23, DSV1, DSV2, and DSV3, are derived from the LM3 habitat variant, LM3-HAB (MCL-H).

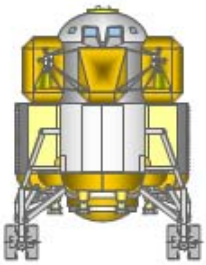

LM1 Personnel Lander – Earth's Moon, Ganymede, and Callisto

LM2 Mars Personnel Lander (MPL)

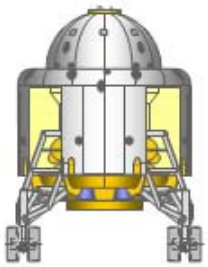

LM3 Mars Cargo Lander-Habitat Variant (MCL-H)

LM4 Personnel Lander – Ceres, Rhea, and Iapetus

LM3/MCL-H* – Inflatable Heat Shield Extension Stowed

LM3/MCL-H* – Inflatable Heat Shield Extension Stowed (Cutaway View)

LM3/MCL-H* – Inflatable Heat Shield Extension Deployed

MCTV Deep Space Vehicle 1 (DSV1)

MCTV Deep Space Vehicle 2 (DSV2)

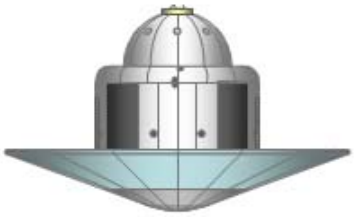

DSV2 – Inflatable Heat Shield Extension Deployed

DSV2 – Inflatable Heat Shield Extension Jettisoned

MCTV Deep Space Vehicle 3 (DSV3)

* LM2/MPL has the same inflatable heat shield extension as that shown in the LM3/MCL-H configurations.

Figure 23. Modular Lander and Deep Space Vehicle Designs for Human Solar System Exploration.

E. Design of Deep Space Vehicle (DSV)

1. DSV Design Overview (DSV1, DSV2, and DSV3)

The DSV design was presented in detail in Ref. 1. It is derived from the LM3-HAB (MCL-H) design of Ref. 6 and also shares common features with the LM2 (MPL) crew lander of Ref 6. For the Mars exploration mission, the DSVs are designed to operate while mated to other vehicles in the MPCV stack, with power provided by solar arrays on the AGM. The DSV Propulsion Stage (PS) is an annular configuration that surrounds the lower part of the Habitat Stage (HS). It utilizes the MPL/MCL central thrust cylinder structure to efficiently carry loads, and is divided into eight bays by shear panels. The DSV HS provides a three-level habitat for the crew, with 67.9m^3 of pressurized volume (habitable volume of 48.5m^3). This provides 24.3m^3 per person for a four-person crew living in two DSVs. The DSV is designed for a three year service life to enable it to perform round trip missions to Mars. DSV1 and DSV2 share the same HS design, and incorporate variations in the designs of their respective PS. The DSV1 PS primary function is propulsion, while the DSV2 PS primary function is storing LSS consumables for the Mars orbit phase. The DSV3 is comprised of a PS with no HS. It utilizes a LIDS Docking Structure (LDS) to enable it to dock with other vehicles at the forward and aft locations. DSV configuration drawings are presented in Figs. 24 and 25, and design data are presented in Table 5. LSS consumables for DSV1 and DSV2 are shown in Fig. 6.

2. DSV Propulsion Section (PS) for DSV1, DSV2, and DSV3

The DSV PS is a modified MPL/MCL Descent Section (DS). Four sets of MPL/MCL landing gear are removed and replaced with a set of three main propulsion system (MPS) fuel, oxidizer, and pressurant tanks in each of the four MPL/MCL DS landing gear bays. Two more MPS tank sets are located in the bays used for cargo on MCL, for a total of 12 main propellant tanks and six pressurant tanks on DSV1/3. The DSV2 PS instead houses six sets of LSS consumables supercritical LO_2 tanks and water tanks and smaller reaction control system (RCS) propellant tanks. The MCL surface docking system (SDS) is removed, and the SDS bay becomes the DSV cargo bay. The MPL/MCL DS aft heatshield and four landing gear doors are replaced by aft-facing plume shields and side-facing thermal blankets on DSV. The DSV1/3 PS retains the eight 13.6 kN (3,042 lbf) MPL/MCL descent engines (throttleable between 38%-100%) as its main engines. Thrust vector control is implemented by differentially throttling the main engines. DSV2 has no main engines. The DSV1/2/3 PS retains the 6-axis RCS of the MPL/MCL DS, which utilizes 16x 745 N (167 lbf) thrusters for attitude control and translation. DSV main engines and RCS thrusters utilize storable, hypergolic monomethyl hydrazine (MMH) and nitrogen tetroxide (N_2O_4) propellants for reliable operation after years of storage. The DSV1 and DSV2 PS both house a personnel airlock and docking hatch in the airlock bay, and an additional docking hatch in the cargo bay opposite the airlock bay. Each docking hatch is equipped with a passive LIDS to permit MPL/MCL landers to dock with DSVs on Mars missions. The airlock and docking ports are accessible by tunnel from the HS. The DSV3 utilizes the DSV1 PS with docking and attach fittings for two MTS-C.

3. DSV Habitat Section (HS) for DSV1 and DSV2

The DSV HS is a slightly modified MCL-H habitat section. It has a spherical forward section, the main crew cabin (upper and middle levels of the three-level pressurized crew cabin), and a cylindrical aft section, a consumables and equipment bay (CEB) carrying life support consumables as shown in Table 6, along with life support system (LSS) equipment, Li-ion batteries, and thermal control equipment. After the TMI burn, the crew transfers from the MPCV to DSV1/DSV2. Water is pumped from water tanks in the DSV1/DSV2 aft CEBs into a 5cm thick water jackets on the inside of the DSV1/DSV2 crew cabin walls, providing the crew with 5 gm/cm^2 of passive hydrogenous radiation shielding against galactic and solar cosmic rays. The cabin wall shield tank is subdivided into many individual cells. The DSV1/DSV2 LSS is modeled after the MPCV system, with a partially closed-loop atmospheric air revitalization system utilizing CO_2 amine scrubbers, and an onboard waste water recovery system that will convert gray water and urine into purified water for drinking, washing, and equipment cooling. Waste water recovery of 85% is required to keep the crew cabin water jacket filled. A backup scenario if the waste water recovery system fails will be to sequentially drain fresh water from the cabin wall shield tank cells and refill them with gray water. The HS upper level has a kitchen/food preparation area, dining area with table and three chairs, study desk with computer workstation, and crew lounge area featuring a comfortable couch, footrests, and an audio/video entertainment center. The HS middle level has crew berthing, with three bunks that can be folded up to make a large exercise area. It also has lockers for clothing, medical equipment, and sanitation supplies. It has separate stalls for a shower and toilet. The HS lower level is located within a cylindrical extension of the main cabin, inside the aft CEB, and is the primary location to house the crew's food stores. An aft docking hatch with passive LIDS enables another DSV or MPL/MCL lander to mate with the DSV. A central ladder runs from the DSV upper docking hatch (with active LIDS), through all levels, to the aft docking hatch.

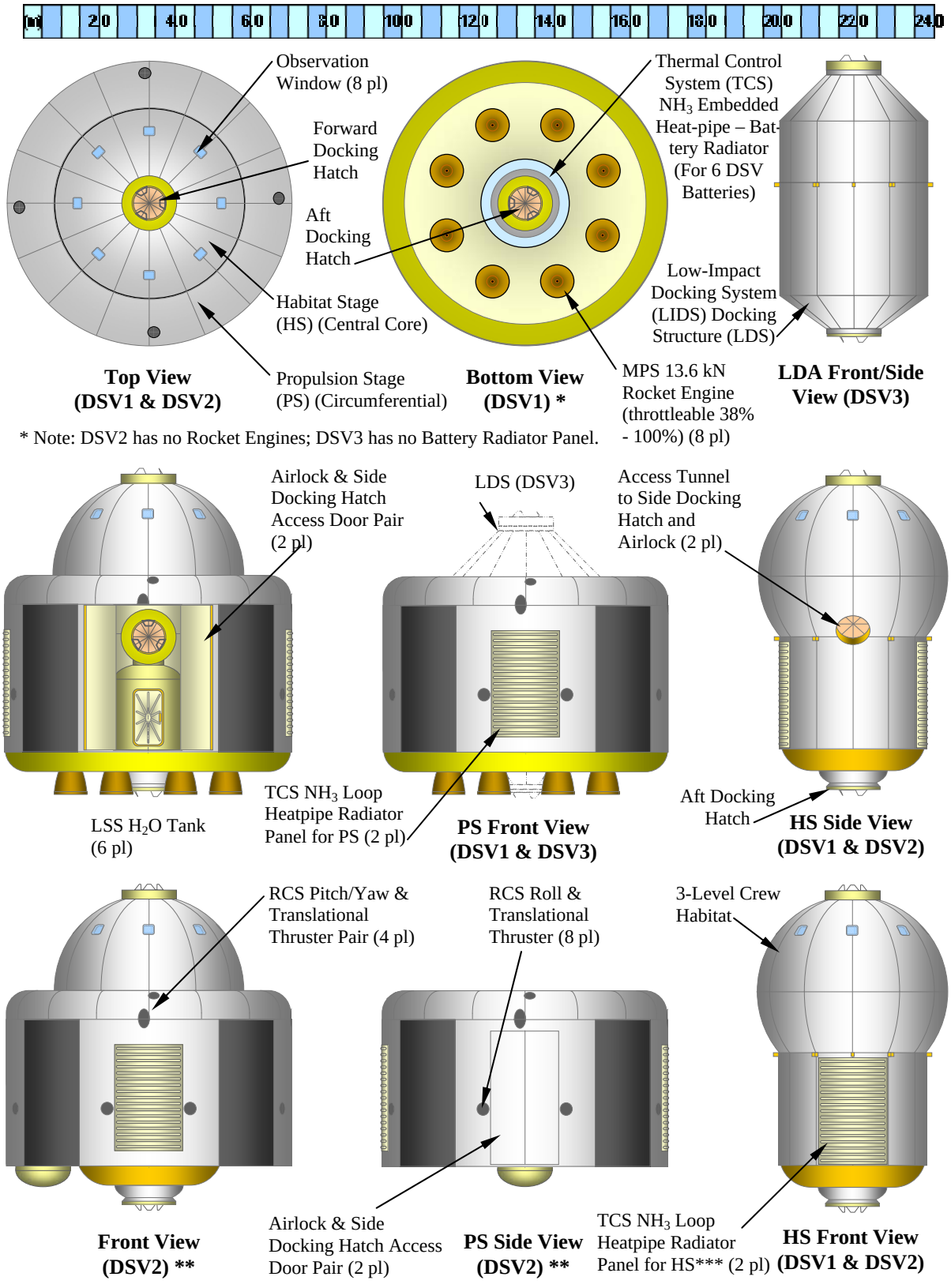

Figure 24. Deep Space Vehicles 1, 2, and 3 (DSV1, DSV2, & DSV3) – Configuration Four-View.

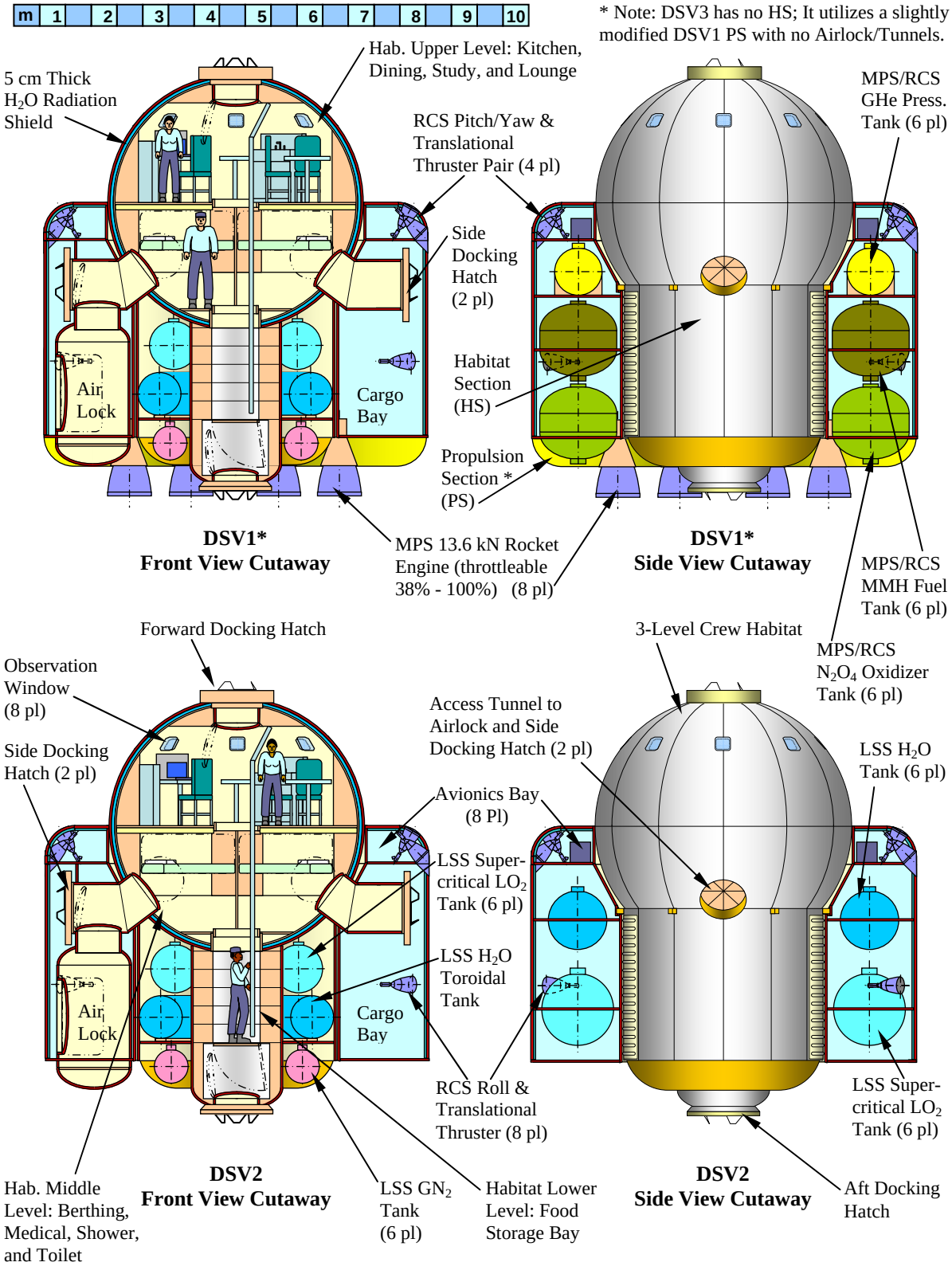

Figure 25. Deep Space Vehicles 1 and 2 (DSV1 and DSV2) – Configuration Front and Side Cutaway Views.

F. Design of Artificial Gravity Module (AGM)

A key feature of the MCTV is its ability to produce artificial gravity (AG) for the crew to prevent deterioration of human tissues caused by prolonged exposure to zero g conditions. The MCTV rotates around its center of mass to induce an outward inertial acceleration or AG ($\alpha = r\,\omega^2$, where α is acceleration, r is the radius to the center of rotation, and ω is the angular velocity). The literature suggests a minimum of 0.2 g_{0E} to provide a minimum level of traction for the crew to perform useful tasks, and maximum rotation rate of 4 RPM to prevent undesirable side effects caused by Coriolis forces. 3.0 RPM is recommended as a compromise between providing adequate AG and minimizing Coriolis forces. The MCTV will provide 0.379 g_{0E} (Mars surface gravity) in the DSV2 living quarters during all flight phases with the following rotation rates: 3.0 RPM (OTO), 3.44 RPM (LMO), and 3.33 RPM (ITO).

The AGM is a key MCTV subassembly with five primary functions: (1) It structurally ties the DSVs and MPCV together to form the MCTV and carries loads between the vehicles during burns and AG operations; (2) The AGM permits crew transfer between DSV1 and MPCV via docking hatches and a pressurized tunnel while DSV1 and the MPCV are docked to the AGM. The need for retractable AGM tunnel segments with sliding pressure seals was avoided by not having continuous inter-vehicle access, with access only at the start and end of the mission and at intermittent times if necessary. The AGM tunnel has sufficient clearance to permit the transit of crewmembers in space suits, if necessary; (3) For MCTV AG rotation, the AGM compensates for changing component vehicle masses throughout the mission, varying its geometry by extending or retracting AG rails to keep the MCTV center of mass/rotation at the AGM de-spun platform (DSP) center of rotation. The AGM must maintain sufficient stiffness in bending and torsion when the AGM rails are fully extended; (4) The AGM provides electrical power and communications during all MCTV flight phases. The AGM DSPs permit solar arrays to track the sun and the high gain Communication Transponder Assemblies (CTAs) to track Earth while the MCTV rotates; (5) The AGM houses the Mini-Mag system. The AGM configuration is shown in Figs. 26 and 27 and its masses are listed in Table 3.

The AGM structure consists of three major parts: (1) the AGM structural tunnel, a 2m diameter thrust cylinder/ pressure vessel with elliptical end domes and a docking hatch at either end. Each hatch incorporates a passive LIDS. The DSV1 and MPCV, each with active LIDS docking hatches, dock with the AGM tunnel when AG rails are fully retracted; (2) extendable/retractable AG rails, with two sets of four each on MPCV and DSV1 sides. AG rails extend and retract to control the position of the MCTV center of mass/rotation, with sufficient (15%) segment overlap at full extension for stability; (3) AG rail-to-vehicle interfaces (RVIs). The MPCV-RVI is a six-legged space frame spanning between AG rails and the MPCV launch abort system hardpoints. Retractable latches secure the MPCV-RVI to six MPCV Launch Abort System attach fittings. The DSV1-RVI is an eight-legged space frame/ring frame assembly spanning between the AG rails and the DSV1 HS cabin and DS thrust cylinder. “Floating” bolts join the ring frame to the HS, to prevent large compressive AGM loads from being reacted by the HS crew cabin during launch of the SLS. Pyrotechnic bolts join the ring frame to the DSV1 DS, so that the DS can be staged with the HS restrained to the AGM. Seven major load cases were analyzed. Four compressive cases were: launch, TMI burns, MOI burn, and TEI burns. During launch and TMI, compressive loads are reacted by the AGM tunnel, the DSV-RVI, and the DSV1 PS thrust cylinder. During MOI and TEI, compressive loads are transmitted between MPCV and DSV1 through the RVIs, AG rails, and AGM tunnel. Three tensile load cases were: hoop and longitudinal stress from the one atmosphere of pressure in the AGM tunnel, and MCTV AG rotation at maximum mass. During AG operations, tensile loads are transmitted between MPCV and DSV1 through RVIs, AG rails, and AGM tunnel.

A concern was implementing solar array sun tracking and antenna Earth tracking on a rotating vehicle. Mounting solar arrays and antennas on DSPs greatly simplifies this problem and eliminates the need for solar array and antenna tracking at 3 RPM. Solar array drive tracking at 3 RPM is not desirable for array drive mechanism longevity, and precise antenna tracking of Earth on a gimbal joint rotating at 3 RPM would be problematic to implement. Vehicle and DSP rotation axes are aligned perpendicular to the ecliptic plane. DSPs are driven by redundant motor/gearbox assemblies and counter-rotate to null AG rotation, providing a stable platform for precise pointing. Accelerometers determine the exact center of rotation to fine tune the CM with AG rail adjustments. Each DSP mounts a pair of 5.5m diameter 6kW Ultra-Flex solar arrays. DC power electronics are contained within each DSP, as well as slip rings to conduct power and ground across rotating joints. The extendable/retractable AG rails conduct DC power and ground between AGM and DSV1/MPCV using slip joints. AG rails are driven by redundant motor/gearbox assemblies. Each DSP also mounts a deep space CTA on an extendable mast. The CTA consists of a radio frequency electronics compartment, antenna feed, high gain antenna reflector, and two-axis gimbal mount. The DSV1 and MPCV communicate with the CTAs wirelessly to eliminate the need for rotating RF joints on DSPs and extendable waveguides/cables on AG rails. The AGM also houses the Mini-Mag subsystem discussed below.

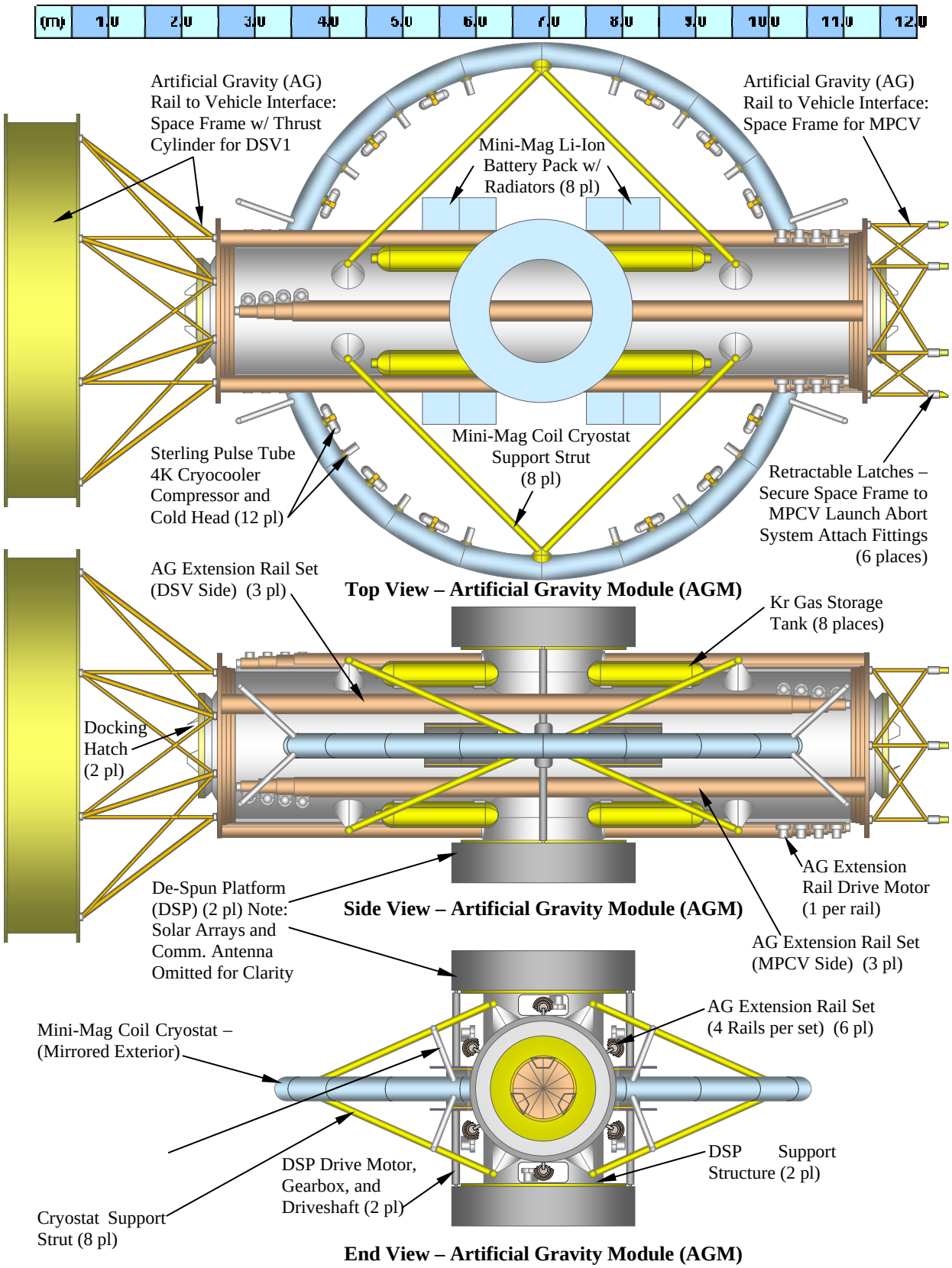

Figure 26. Artificial Gravity Module (AGM) – Configuration Three-View.

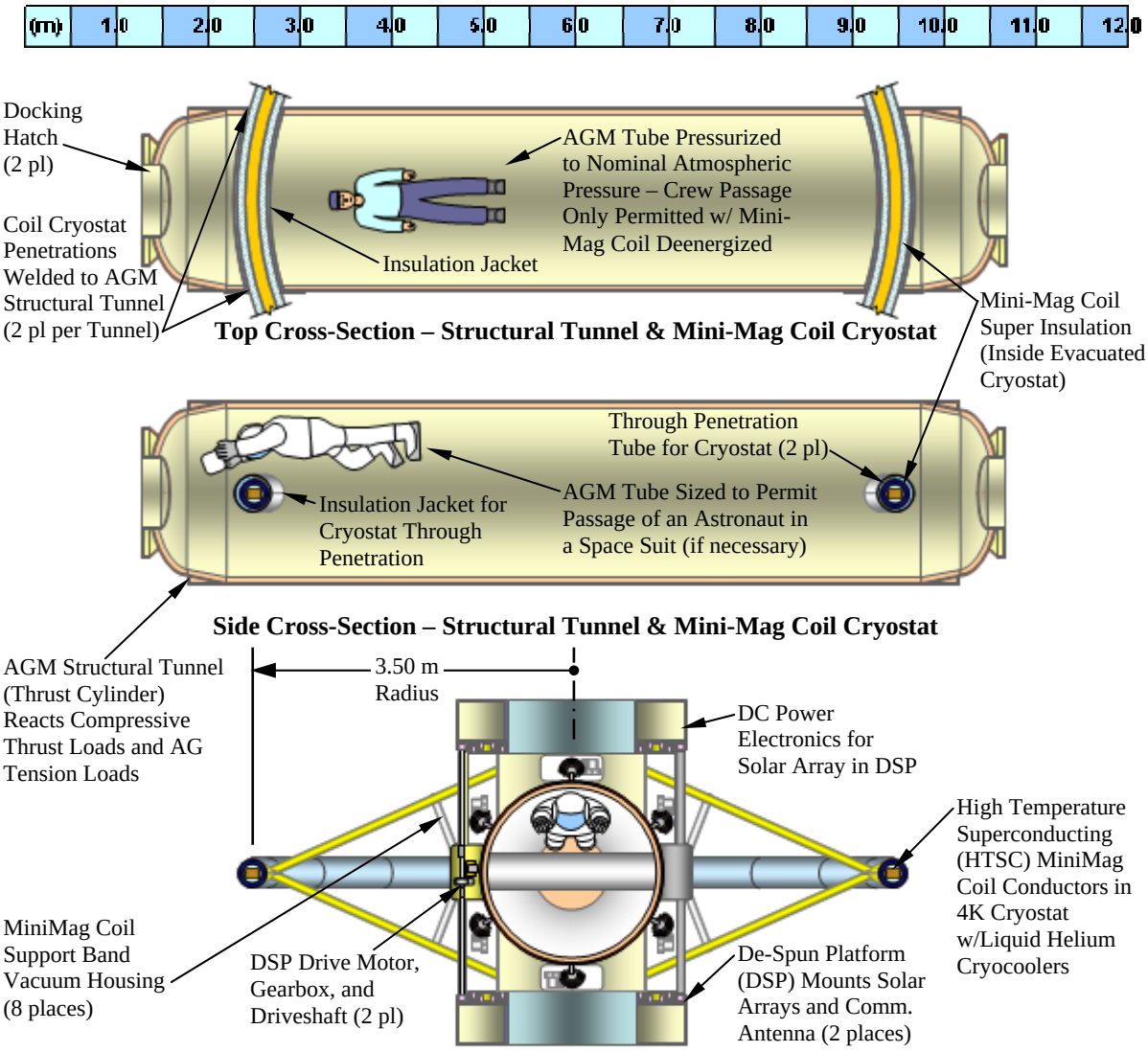

Figure 27. Artificial Gravity Module (AGM) – Configuration Cross-Section Views.

VI. Design of Mini-Magnetosphere (Mini-Mag) Electromagnetic Radiation Shield

A. Overview

The basic concepts underlying the shielding possibilities afforded by creating a plasma-charged magnetosphere around a spacecraft were described at some length in Ref. 1. The section therein on the design of the coil system to produce the required magnetic field elaborated the optimization of the range of the bow-shock or magnetopause (at which the solar wind ram pressure is essentially balanced by the magnetospheric magnetic field pressure) with respect to the total mass required for the coils, supports, insulation, cryocoolers, cryogens etc. This showed that given the criterion of mass minimization, it is best to choose a simple flat round coil, with the largest possible radius that will fit within the launch vehicle envelope, producing a simple dipole field structure resembling that of the Earth.

In that earlier design, it was conjectured that the use of pressurized neon at ~28K would facilitate the use of a high-temperature superconductor design solution while minimizing the power required for the cryocoolers. It was proposed that a set of cryocoolers would cool the periphery of the coil winding and that a bath of liquid neon would ensure an adequate distribution of the cooling around the winding. In the variation presented in this paper, the use of a high temperature superconductor (HTS) is retained but since the cryocooling requirement was quite small in the previous version, the option of moving to helium temperatures ~4K and exploiting the ability of the HTS to tolerate extremely large magnetic fields has been explored. This permits the coil cross-section to be markedly reduced, saving considerable weight in the coil structure while marginally respecting the operating capability of HTS conductors already proven in the laboratory. In addition, the design now features contact cooling only, so that it is no longer necessary to have a large pressurized gas tank to hold the neon inventory when not in the cryostat.

There remain many questions about the physical behavior of the Mini-Mag, which cannot be addressed until the modeling has been developed significantly, some of which are listed in the section of this chapter on possible future studies, and so for the moment it has been assumed that the dipole field strength of the magnet described in Ref. 1 should be preserved as the design evolves. (This gave estimated bow-shock radii of 720m for the “low normal” solar wind ram pressure of 3nPa, falling to 170m for a 16nPa “severe solar storm” case.) Re-examination of the available space in the launch vehicle has allowed the diameter of the current centroid to be increased from 6.0 to 7.0m, permitting a reduction in total amp-turns from 5.6MAt to 4.1MAt while keeping the (long-range) dipole strength as before. The resulting magnetic field at the centre of the coil is accordingly 0.74T and the field experienced by the crew, at >8m from the coil center (DSV1 crew cabin upper level ceiling, with AG rails retracted to a designated minimum position for crew safety during MiniMag operation) is <62mT, still well below the 200mT recommended maximum continuous exposure of the International Commission on Non-Ionizing Radiation Protection. The new design considers in greater depth the details of the winding pack construction, including insulation, a strong-back (bonded to the winding) and strong but low thermal conductivity supports. A number of significant weight savings have accordingly been identified, as described in the summary of this section of the paper, totaling 1.44t.

B. Design of Electromagnetic Coil

Previously the coil was considered to be wound with a high proportion of internal support structure, insulation, and thermal conduction plates, but with scant attention to the actual winding design. In this new version, it is assumed that the HTS conductor (which resembles a tape, 12mm wide and 0.1mm thick, almost entirely composed of steel and copper and with only ~3μm of actual HTS material) is wrapped in “2 mil” Kapton tape for insulation, arranged to average an additional “4 mil” or 0.1mm per HTS conductor layer.

Recovering the previous dipole strength which is given by IA, the total current times the area enclosed by the coil, of 158MA*m^2, leads to a total amp*turns of 4.115MAt in the new R_0 = 3.5m coil. At 700A conductor current, the same as in the previous design but now at 4K (permitting a maximum magnetic field strength of ~17T in conductors available today) instead of ~28K, this requires 5878 turns. Allowing a total cross-sectional area for each turn (including insulation) of 12mm x 0.2mm, the total winding pack area becomes 141cm^2, half of it made of Kapton (density 1.42g/cc) and the other half HTS conductor tape (density ~8.3g/cc).

It is proposed that the winding is produced in double pancakes (clock-springs) with the innermost turn providing the transition between the two pancakes. Each double pancake is thus 24mm thick, taken as 25mm to allow for insulation thickness and some winding tolerances. As in the previous design, it is intended to divide the overall winding into two halves, separated by a robust septum plate (e.g. titanium alloy, density 4.51g/cc), to confer a 50%

operability with the coil or its cryogenic or power supply systems damaged in some way. Accordingly, there must be the same number of 25mm thick double pancakes on each side of the septum, giving a 50mm modulus for the overall winding pack thickness (50, 100, 150…mm). The titanium plate is 2mm thick, sandwiched between two 1mm thick pure aluminum plates (density 2.7g/cc) to assist thermal conduction into the core of the winding. The present design solution is to have two 25mm thick double pancakes each side of the 4mm thick septum, separated by additional 1mm thick aluminum thermal conduction plates, developing an axial total of 106mm and requiring a radial dimension of ~14cm to produce the necessary 141cm2 of winding pack area. The masses of the various components of the new design are shown in Table 10, and the MiniMag coil details are shown in Fig. 28.

Table 10. MiniMag System Mass Breakdown

Mass (kg)	Old Design	New Design	Mass Saved
HTS Conductor Tape	1,304	1,286	
Kapton insulation	0	220	
Aluminum thermal conduction plates	0	33	
Titanium septum plate	0	28	
Balance of winding pack	1,304	0	
Cryostat casing (10bar)	77	0	
Cryostat casing [1]	0	150	
Coil strong-backs/cold plates	0	192	
Coil supports (8 off bands & tubes)	0	160	
Cryocoolers	110	130	
Cryostat superinsulation	270	77	
Superinsulation casing	23	0	
Superinsulation lining and 60K thermal shield	0	20	
Cryogen storage tanks	107	0	
Seed gas storage tanks	107	125	
Coil energy storage batteries	142	103	
Battery radiator panels	9	8	
Mini-Mag coil housing	143	0	
Mini-Mag control system [2]	17	20	
Dry mass margin (15%)	542	383	
Cryogen (neon gas)	216	0	
Seed gas (krypton gas)	250	250	
Total Mass, Mini-Mag System	**4,621**	**3,185**	**1,436**

[1] One bar plus strengthening near AGM Pressurized Structural Tunnel (PST) for MiniMag coil support tubes.
[2] Control system, cabling, tubing, seed gas nozzles and valves, etc.

Using the conservative approximation that the highest magnetic field in the winding pack will be approximately equal to the field around a straight filamentary conductor at a radius equal to the half-width of the winding pack, 53mm in the narrower direction in this case, leads to a peak magnetic field of 15.5T. This is possible at 4.2K with HTS conductors already available and falls well within supplier forecasts for imminent HTS developments.[17] The connections between adjacent pancakes will be resistive, since there is presently no way of joining HTS conductors together with a superconducting joint. Typically the actual HTS layer, a few microns thick, is laid via interface layers onto a steel tape, coated with further interface layers and then both sides of the tape are coated with copper. Thus the lowest resistance joints are achieved by soldering the faces nearest to the HTS layer together. The resulting joints benefit from being at cryogenic temperatures but still introduce some local Ohmic heating and for this reason are, when possible, located on the surface of the winding pack near a source of cooling.

Of much greater concern are the four 700A current feeds from the ambient surroundings, which will be much colder than is typical on Earth but still very much hotter than 4K. Here an ambient temperature of 180K is assumed. Clearly since the free electrons in a metal conduct heat energy just as well as they conduct electrical current, there is no “obvious” design approach that limits the thermal input while minimizing the electrical resistance. The heat flow into the 4K region due to thermal conduction from the exterior and/or the heat generated in the feeder itself is estimated to be of the order of 200W to the ~60K heat shield, which correspond to ~2kW electrical power required for the cryocoolers to remove it. Further optimization of the current leads is one of the outstanding issues for future work on this design, not least the connection from the 60K point to the 4K coil. This is usually only tens of mW for

currents of ~1kA but is facilitated by HTS conductors operating in a region with much lower magnetic field than is envisaged immediately around the Mini-Mag coil.

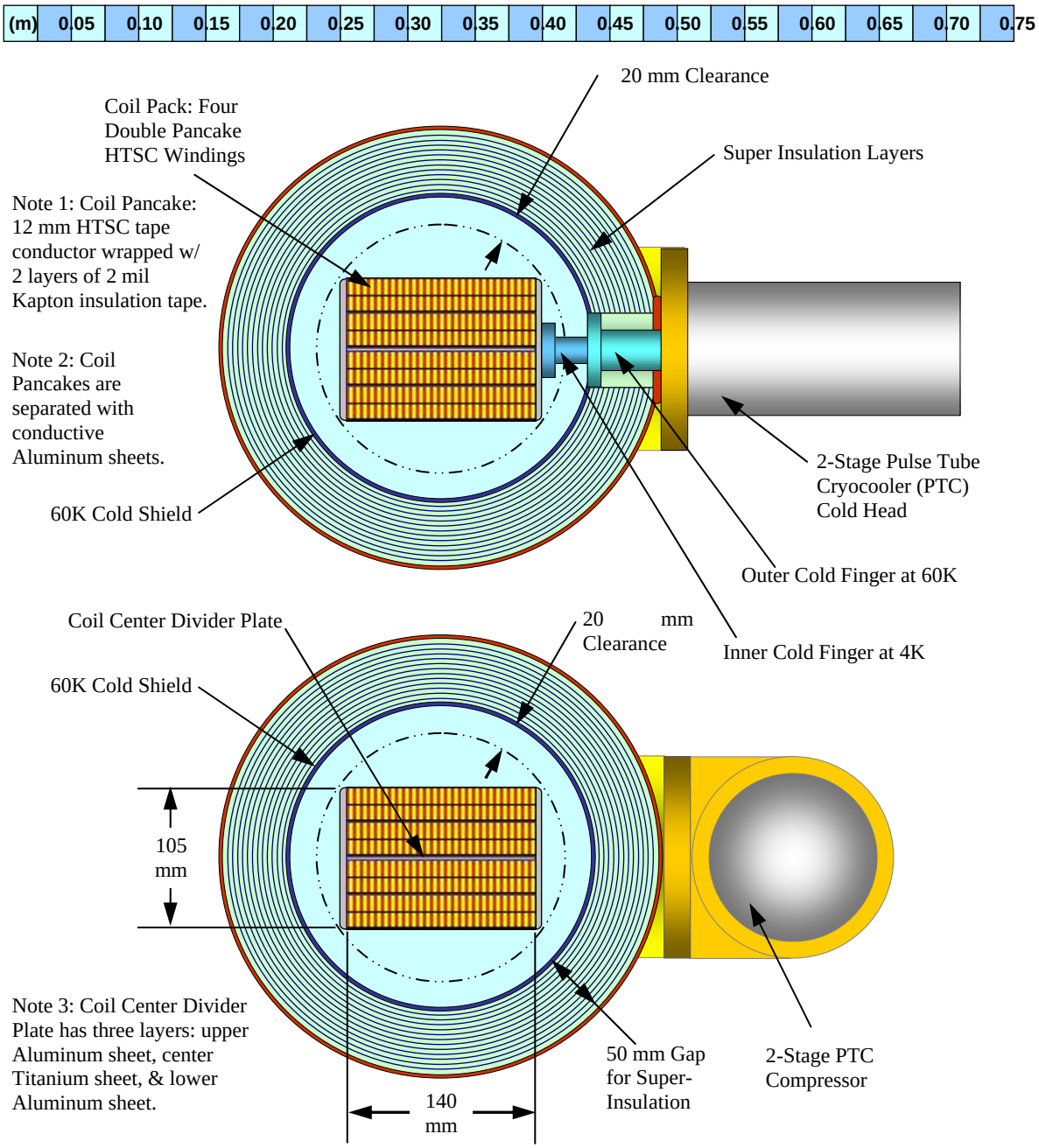

Figure 28. Mini-Mag Coil Cross-Sectional Details: Conductor Windings, Cryostat, Insulation, and Cryocoolers.

C. Cryostat and Coil Supports

One significant change from the previous design is that it is now considered necessary to evacuate the superinsulation in the period before launch when the coil is at operating temperature but not energized. This means that the cryostat has to resist full atmospheric air pressure and accordingly has to be of somewhat higher mass. As noted in Ref. 1, superinsulation works best in its high temperature range, near ambient, when the mirrored surfaces inhibit radiative heat transfer and the thermal conduction through the layers is of much lesser significance. At cryogenic temperatures, especially towards ~4K as now proposed here, radiative transfer becomes insignificant and

the finite thermal conduction of the superinsulation can be obviated by introducing a low-emissivity heat shield, held at ~60K by thermal connection to an intermediate stage in the cryocoolers. This is depicted in Fig. 28.

In the earlier work, there was no detailed consideration of the supports of the ~28K winding pack within the superinsulation encapsulation or the cryostat, with an implication that this could be achieved by hard contact pads made of a thermally insulating material and distributed around the winding as necessary. In this paper, the supports have been considered more fully and it is recognized that to keep the heat loads down on the winding, now reduced to ~4K which makes the Carnot efficiency more challenging, insulating support blocks are not sufficient. Borrowing a concept from the AMS satellite magnet development[18] the intention is now to support the coil (via a strong-back ring attached to it) from pre-tensioned bands of carbon fiber and glass fiber, as shown in Fig. 29. These can provide a strong, if not rigid, support against operational forces (dominated by launch accelerations of a few g) while exhibiting very small thermal conduction.

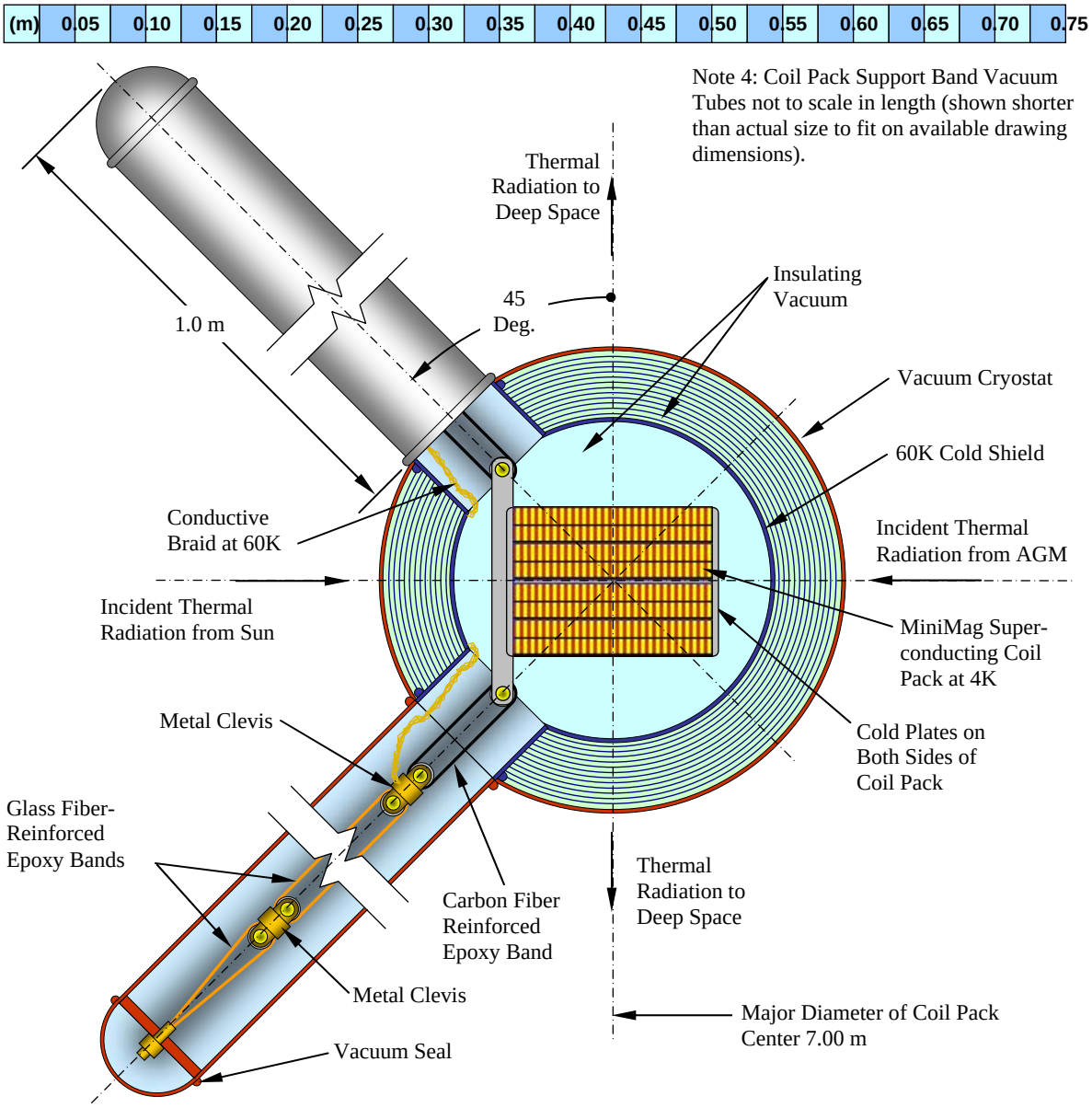

Figure 29. Mini-Mag Coil Cross-Sectional Details: Conductor Windings, Cryostat, Super Insulation, and Supports.

The support bands cover the full temperature range from 4K to 180K and therefore have to be placed within evacuated housings in order to function properly as thermal breaks. As shown in Fig. 25, they are located near the pressurized support tunnel within housings 1m long, and are themselves supported by the outer shell of the cryostat around the coil and its superinsulation. This means that the cryostat, at least in the region where it transfers these support loads to the AGM pressurized structural tunnel, must be strong enough to stand off the launch acceleration loads on the coil as well as air pressure (before and during the early part of the launch).

D. Energy Storage and Balance of Plant

Previously the energy stored in the coil (considered as one assembly) was estimated to be 235MJ but since the current necessary for the same long-range dipole strength drops like the coil radius squared, while the inductance is essentially only linear with radius, the inductively stored energy has also reduced in the new design, to ~148MJ. This energy is stored in batteries whenever the coil is not energized and accordingly the new design (assuming the same specific energy capability for the batteries as before) needs a battery mass of 103kg, 60kg less than previously.

As shown in Table 10, most of the aspects of the Mini-Mag system not reconsidered in this paper have been assumed to have the same mass as before, although now the Mini-Mag housing, a heat and micrometeoroid shield previously placed around the outside of the cryostat, has been obviated by the increased thickness of the cryostat. The removal of the housing helps to reduce the mass but the thicker cryostat, newly introduced 1m long coil-support tubulations and the strong-back on the winding pack largely offset this saving. Even so, as the table shows, a considerable overall mass reduction has been achieved in the design compared to that of Ref 1.

E. Future Considerations

These naturally fall into two groups, one for the engineering aspects of the coil and the other for the physics issues (the resolution of which will ultimately determine the overall engineering requirement, of course). The lists shown below are, at this stage, more illustrative than exhaustive.

Engineering developments:

- change the coil design to the class with current parallel to the magnetic field, in order to exploit the considerable improvement thus conferred in maximum current capability of high temperature superconductors for a given magnetic field strength and operating temperature[17], and to exploit a “force-free” configuration,
- alter the long-range dipole strength (IA) if physics modeling suggests that this is necessary,
- optimize the current feeds e.g. regarding length, diameter, variation of diameter along length, and choice of material,
- check the dynamic loads on the winding pack supports during launch and optimize the overall mass, aiming for a total heat load of (say) 5% of that of the current feeds,
- find a design solution for cryocoolers capable of operating in the ~16T magnetic field near the winding (e.g. variants with no moving metallic parts),
- refine the total 60K and 4K cryocooler mass and power requirements,
- optimize the mass total of the insulation and cryoplant,
- consider introducing coil movement stops of limited compliance to prevent overload of the coil support bands by off-normal accelerations (e.g. during launch),
- analyze the safety aspects such as system behavior given predictable faults, in order to identify design requirements regarding sub-system redundancies, control and instrumentation implications etc.

Physics modeling developments:

- agree a nominal prescription of the incident particle species mix, energy distribution, intensity, event duration, interval between events and total number of events in the intended mission,
- agree the permissible mission-total radiation dose for the astronauts,
- determine the minimum dipole strength required for the MiniMag,
- estimate the effects of residual “auroral” particle flow into the polar regions of the MiniMag,

- calculate the minimum electron density required for the plasma in the MiniMag to provide an effective attenuation and deflection of the worst-case incident ions,
- estimate the temperature or mean energy that the plasma seed ions acquire, since this is critical to assessing their residence time (and hence required launch mass) considering their thermal velocity, collisionality and finite beta (plasma pressure over magnetic field pressure),
- clarify the plasma physics phenomenology in the region where the beta of the MiniMag plasma (ionized seed gas plus acquired solar wind particles) exceeds unity,
- check whether or not there are significant unintended effects arising from the deployment of the MiniMag, such as torque induced on the spacecraft by the dipole field interacting with the interplanetary field, or a solar sail effect from the large area of solar wind being intercepted.

VII. Enabling Technologies

Continued development of key enabling technologies is needed to enable human exploration of Mars:

(1) Heavy lift launch vehicles, such as the SLS, capable of injecting large payloads (130 metric tons) into LEO.
(2) Deep space exploration vehicles capable of supporting humans on long-duration missions of up to 32 months, with large δV capability and sufficient habitation volume for crew members (e.g. DSV1 and DSV2 on MCTV).
(3) Deep space exploration vehicles that can provide artificial gravity for crewmembers on long-duration missions to prevent deterioration of human tissues caused by prolonged exposure to zero g (e.g. the MCTV with AGM).
(4) Highly reliable retention systems for long-term, low-loss storage of cryogenic liquid oxygen and liquid hydrogen propellant for a seven month outbound transit to Mars.
(3) Highly reliable retention systems for long-term, low-loss storage of cryogenic liquids (supercritical LO_2 and LN_2) for life support consumables for a 30 to 32 month duration Mars mission.
(5) Reliable, lightweight, and durable habitation and exploration equipment for long-duration missions, including space suits, manned maneuvering units, communications equipment, and scientific instruments.
(6) Passive radiation protection, including the use of life support consumables for shielding and the development of reduced weight “dual-mode” composite materials for structures that incorporate radiation protection.
(7) Active radiation protection: the Mini-Magnetosphere electromagnetic radiation shield to protect crews from the extreme GCR and SCR radiation hazards could be a key enabler for human interplanetary exploration.
(8) Large (up to 30m dia.) supersonic DGB parachutes to enable Mars landers in the 21t MPL/MCL mass range.
(9) Lightweight, inflatable, ablative heatshield structures for MPL/MCL-type inflatable heatshield extensions.
(10) Precision landing systems for Mars landers, including aerodynamic steering, active terrain sensing, and powered descent steering and guidance to permit crew landers to rendezvous with pre-positioned assets on the surface.
(11) Support equipment for long-duration human habitation and exploration on the surface of Mars, including habitats, space suits, rovers, nuclear power generators, solar arrays, communications gear, and scientific equipment. This will enable the crew to conduct extensive and detailed scientific explorations of Mars.
(12) In-situ resource utilization processing equipment, which would significantly reduce the mass of consumables needed to be transported from Earth to Mars and increase the scientific payload capability of the mission.

VIII. Conclusion

This paper presents a conceptual vehicle architecture for human exploration of Mars, the Mars Exploration Vehicle (MEV) architecture. The MEV provides key features that will be needed to keep the crew healthy and safe during a ~30 month duration round-trip mission to Mars: sufficient volume for human habitation, artificial gravity to prevent deterioration of the human body caused by prolonged periods in microgravity, and effective passive and active crew biological shielding from solar and cosmic radiation to prevent radiation sickness. The MEV architecture utilizes aerobraking at Mars to minimize IMLEO thereby minimizing the number of launches required to assemble the MEV and the associated launch costs. It uses a minimum number of straightforward docking events to simplify assembly of the MLTV and MCTV in the low Earth parking orbit. It extensively makes use of existing or near-term technology to minimize development cost and risk, and utilizes the existing capabilities of current launch facilities for the SLS and Delta IV Heavy. The MEV architecture is flexible and modular, and can be used on shorter duration human exploration missions to lunar orbit and NEO asteroids before being used on missions to Mars. Its use on these precursor missions will demonstrate key technologies and reduce risk for the longer duration Mars missions. The Mini-Magnetosphere concept for active crew biological radiation shielding has significant promise, as a key enabler for human interplanetary exploration, affording the crew effective protection from the interplanetary radiation environment. Ref. 1 and this paper have demonstrated compelling arguments for its further development.

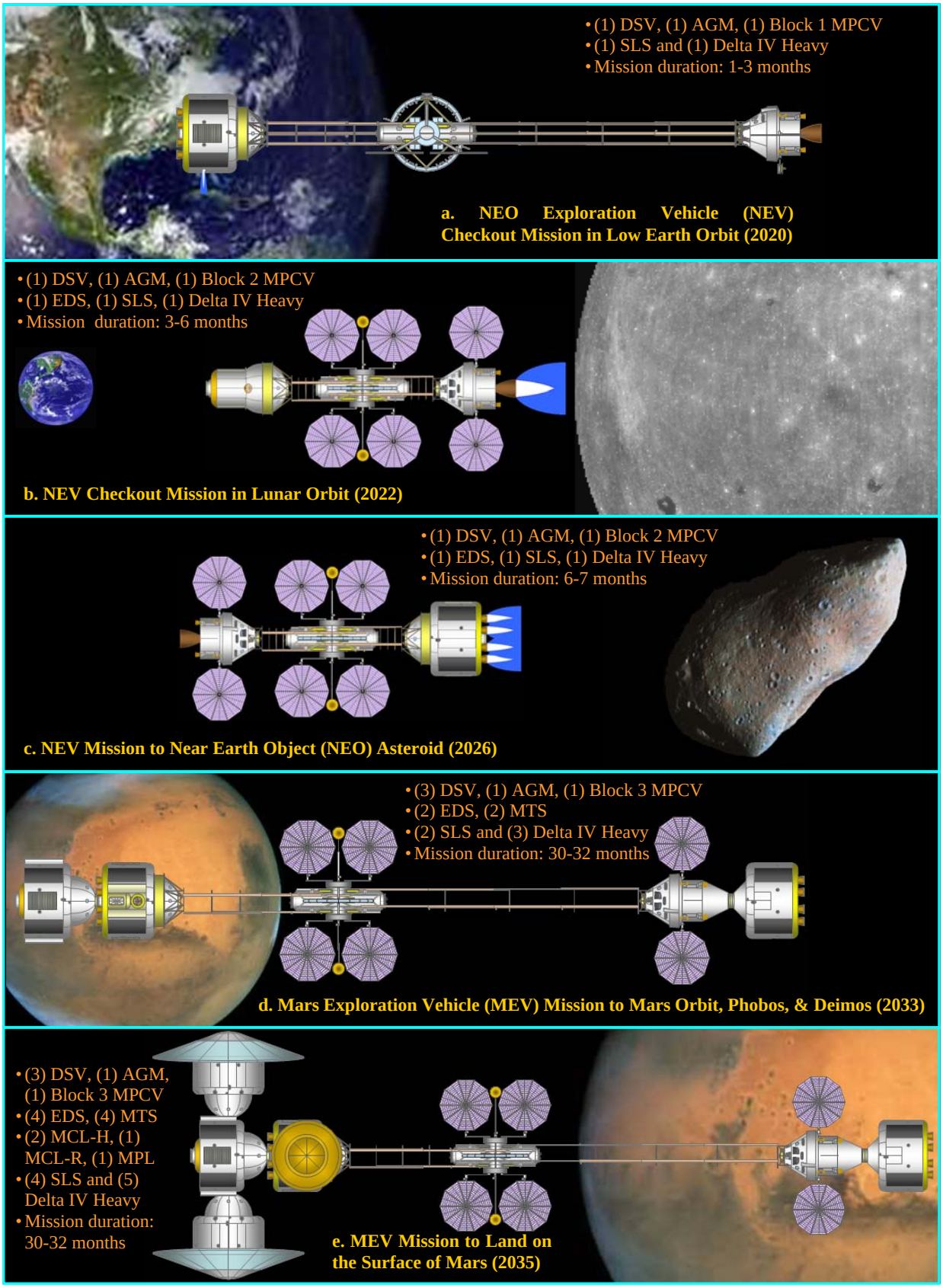

Figure 30. Flexible Path Missions Enabled by the Modular Mars Exploration Vehicle Architecture.

References

[1] Benton, Sr., M. G., Bamford, R.A, Bingham, R., Todd, T., Silva, L., and Alves, P., "Concept for Human Exploration of NEO Asteroids using MPCV, Deep Space Vehicle, Artificial Gravity Module, and Mini-Magnetosphere Radiation Shield," AIAA-2011-7138, 44th AIAA SPACE 2011 Conference & Exposition, Long Beach, California (2011).

[2] Bamford, R., et al., "The interaction of a flowing plasma with a dipole magnetic field: measurements and modeling of a diamagnetic cavity relevant to spacecraft protection," Plasma Physics and Controlled Fusion, Vol. 50, 12, 124025, Dec. 2008.

[3] Hopkins, J. B., Pratt, W. D., "Comparison of Deimos and Phobos as Destinations for Human Exploration and Identification of Preferred Landing Sites," AIAA 2011-7140, 44th AIAA SPACE 2011 Conference & Exposition, Long Beach, CA (2011).

[4] Woodcock, Gordon, "Designing an Enduring Mars Campaign," AIAA-2011-7214, 44th AIAA SPACE 2011 Conference & Exposition, Long Beach, California (2011).

[5] Benton, Sr., M. G., "Spaceship Discovery – NTR Vehicle Architecture for Human Exploration of the Solar System," AIAA-2009-5309, 45th AIAA/ASME/SAE/ASEE Joint Propulsion Conference and Exhibit, Denver, Colorado (2009).

[6] Benton, Sr., M. G., "Crew and Cargo Landers for Human Exploration of Mars - Vehicle System Design," AIAA-2008-5156, 44th AIAA/ASME/SAE/ASEE Joint Propulsion Conference and Exhibit, Hartford, Connecticut (2008).

[7] Smith, J. C., and Bell, J. L., "2001 Mars Odyssey Aerobraking," AIAA 2002-4532, AIAA/AAS Astrodynamics Specialist Conference and Exhibit, August 2002, Monterey, California (2002).

[8] Gladden, R. E., "Mars Reconnaissance Orbiter: Aerobraking Sequencing Operations and Lessons Learned," SpaceOps 2008 Conference (Hosted and organized by ESA and EUMETSAT in association with AIAA), AIAA 2008-3353.

[9] Johnston, M. D., Esposito, P. B., Alwar, V., Demcak, S. W., Graat, E. J., and Mase, R. A., "Mars Global Surveyor Aerobraking At Mars," AAS 98-112 (1998).

[10] Mottinger, B., "Aerobraking: Mars Global Surveyor and Further Analysis of Aerobraking Options," ASEN 5050 Space flight Dynamics Course, Fall 2000 (online reference).
URL http://ccar.colorado.edu/asen5050/projects/projects_2000/mottinger/ [cited 8/12/2011].

[11] Schaffer, M., "A Study of Cryogenic Propellant Stages for Human Exploration Beyond LEO," IEEE 2012, March 2012

[12] Zegler, Frank, "An Integrated Vehicle Propulsion and Power System for Long Duration Cryogenic Spaceflight", AIAA 2011- , September 2011

[13] Kutter, B. F, "Atlas Centaur Extensibility to Long-Duration In-Space Applications", AIAA 2005-6738, September 2005

[14] DeKruif, J., " Centaur Upperstage Applicability for Several-Day Mission Durations with Minor Insulation Modifications", AIAA-2007-5845, September 2007.

[15] Benton, Sr., M. G., "Crew Exploration Lander for Ganymede, Callisto, and Earth's Moon - Vehicle System Design," AIAA-2009-5179, 45th AIAA/ASME/SAE/ASEE Joint Propulsion Conference and Exhibit, Denver, Colorado (2009).

[16] Benton, Sr., M. G., "Conceptual Design of Crew Exploration Lander for Asteroid Ceres and Saturn Moons Rhea and Iapetus," AIAA-2010-0795, 48th AIAA Aerospace Sciences Meeting, Orlando, Florida (2010).

[17] Lehner, T., and Zhang, Y. "Development, Manufacturing and Applications of 2G HTS Wire at SuperPower," Center for Emergent Superconductivity – Workshop at University of Illinois, Urbana, IL, November 2011;
URL http://www.superpower-inc.com/system/files/2011_1108+CES+Workshop_+TL_YZ.pdf [cited 15 December 2011].

[18] Stafford-Allen, R., "A Review of the AMS Magnet – Mechanical Overview and Status," AMS Technical Interchange Meeting, Center for Advanced Space Studies, Houston, October 2004;
URL: http://ams.cern.ch/AMS/Reports/TIMOct04/MagnetStatus_RCSA1.ppt [cited 16 December 2011].